Alma Mater Studiorum · Università di Bologna

Scuola di Scienze

Dipartimento di Fisica e Astronomia

Corso di Laurea Magistrale in Fisica

In vivo and in vitro simulation of a passive intra- aortic dumper

Relatore:

Prof. Romano Zannoli

Presentata da:

Michela Olivieri

Correlatore:

Dott. Ivan Corazza

Anno Accademico 2017/2018

Sommario

In molte situazioni critiche cardiovascolari si ricorre all'utilizzo di un sistema di supporto meccanico, la contropulsazione aortica (IABP). La IABP si basa sul gonfiaggio e sgonfiaggio di un palloncino posto all'interno dell'aorta, per produrre una riduzione del carico ventricolare durante la sistole e un miglioramento della perfusione coronarica durante la diastole.

Alcuni problemi legati all'IABP sono tuttora irrisolti: elavato costo, inefficacia in caso di aritmie ed eccessiva sollecitazione meccanica della parete arteriosa per il rapido gonfiaggio e sgonfiaggio del palloncino.

A questi problemi esiste una possibile soluzione: la contropulsazione passiva (PIABP), che non utilizza una fonte di energia esterna ma sfrutta la residua funzionalità cardiaca ottimizzando l'adattamento meccanico ventricolo-aorta dal punto di vista energetico.

L'obiettivo iniziale di questo lavoro era la validazione clinica della PIABP, su pazienti, con l'aggiunta della misura dei flussi aortici per confermare il risultato di un precedente lavoro. Durante la sperimentazione effettuata su due pazienti sono emersi problemi legati alla tecnica strumentale impiegata per rilevare i segnali di flusso, che si è mostrata troppo operatore-dipendente. Per questo motivo l'attenzione si è spostata sulla validazione a banco, al fine di confermare gli effetti della PIABP sulla riduzione dell'ampiezza del polso aortico e valutare anche le variazioni della pulsatilità di parete vascolare. Questo effetto può, infatti, favorire

l'aderenza di protesi endovascolari alla parete del vaso, rendendo il PIABP una possibile soluzione ad un problema clinico emergente. Per effettuare queste valutazioni sono state associate misurazioni di tipo meccanico (pressioni e flussi) e di tipo ottico (videocamera) implementando un sistema assolutamente originale.

Abstract

In most critical cardiovascular situation it's necessary to use a supporting mechanical system: the aortic counterpulsation (IABP). IABP consists in inflation and deflation of a balloon positioned in the aorta, with a decrease of the ventricular load during systole and an improvement of coronary perfusion during diastole.

Nevertheless some problems related to IABP remain unsolved: high cost, controversial effect in presence of cardiac arrhythmia, excessive mechanical solicitation of the arterial wall due to rapid balloon inflation and deflation.

It's possible to solve these problems with a passive counterpulsator (PIABP), that doesn't need energy from outside and exploits its functionality optimizing aorto-ventricular energetic matching .

The initial aim of this thesis was the clinic validation of PIABP on patients, adding the aortic flows measurement to confirm the results of a previous work. During the test on two patients some problems arose, due to intra operator's variability.

For this reason the work has been shifted on validation on bench, to confirm the effect of PIABP on energy transfer and mechanical efficiency improvement. For these evaluations, an optical monitoring has been joined to the mechanical one (pressures and flows) by implementing an absolutely original system. This optical possibility allows to link the pressure pulsatility to the vascular wall movements and to face a new clinical problem: superficial adaptation of endoprothesis to the

vascular wall. The PIABP may be used as an instrumental tool in these procedures and opens a new perspective for Medical Physics.

Contents

Introduction

This thesis is focused on passive counterpulsation (PIABP), as a possible solution to some unsolved problem of the active counterpulsation. PIABP can improve the mechanical matching between ventricle and aorta without external energy use, so the functional benefits are based on a more efficient management of the energy just produced by the ventricle.

The initial aim was the clinic validation of PIABP on patients, adding the aortic flows measurement to confirm the results of a previous work. Two patients were recruited and studied but the flow measurements show an high intra-operator's variability making it impossible to correctly quantify the aortic values.

So the goal of the present work was moved on on-bench validation of the PIABP focusing on the evaluation of the aorta pulsatility. The reason of this choice was to face a new clinical problem: the superficial adaptation of endoprothesis to the vascular wall. In fact, one of the main problem related to the endo vascular prothesis insertion is the endoleak phenomenon: the passage of fluid between the prothesis and the arterial wall, rendering the therapeutic intervention inefficient. Our hypothesis is that a reduced pulsatility due to PIABP can improve the superficial adaptation of endoprothesis to the vascular wall avoiding the endoleaks.

The first section of this thesis is focused on a theoretic introduction and an analysis of physical and biomechanical principles to describe the matching be-

tween ventricle and aorta. The second section describes the active intra-aortic balloon pump with its benefits and its related problems. To solve these problems is introduced the passive counterpulsation with its goals also on the prothesis insertion. In the third chapter the in vivo testing is described. The fourth section contains the description of the on-bench simulation, the experimental protocol and the results. The fifth chapter reports discussion and conclusions.

Chapter 1

Medical and biomechanical contents of cardiovascular system

1.1 Macroscopic anatomy of the heart and the circulatory system

The heart is a muscular pump connected with cardiovascular system. The main role of the heart is to maintain an appropriate circulation of blood at the level of the organs, at rest and during exercise. The heart has four chambers, two atria and two ventricles, that are connected by heart valves; these valves prevent the backward flow of blood and keep it moving in the right direction.

The atria receive blood coming back to the heart and then fill ventricles with blood during ventricular relaxation; they are separated by a thin interatrial septum into the left atrium and the right atrium.

The ventricles are responsible for pumping blood to the entire body and they are divided by the interventricular septum. The left ventricular myocardium is thicker than the right because the pressure generated by the left ventricle is greater

than that generated by the right. The atrioventricular valves (AV) are thin structures that separate the atria and ventricles; in particular the mitral valve is bileaflet and is located between the left atrium and left ventricle, while the tricuspid valve is a trileaflet valve that separate the right atrium and the right ventricle.

The semilunar valves separate the ventricles from the arterial chambers, in particular the aortic valve is located between the left ventricle and aorta, while the pulmonary valve separates the right ventricle from the pulmonary artery.

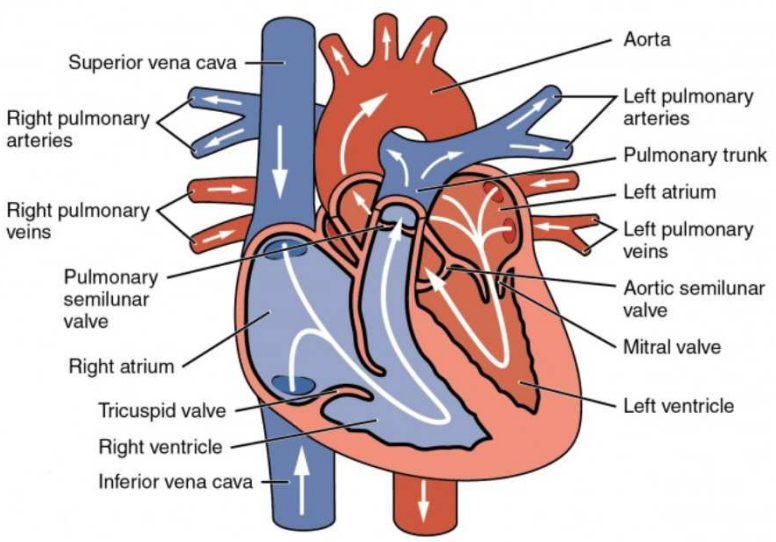

Figure 1.1: Heart anatomy

The circulatory system is composed of two distinct circuits: the pulmonary circuit and the systemic circuit. The pulmonary circulation involves blood transfer to and from the heart and lung, while the systemic circulation deals with the whole body.

Deoxygenated blood enters into the right atrium via two large veins: the superior and inferior venae cavae. When the right atria contracts (atrial systole), blood flows into the right ventricle, through the tricuspid valve.

During the contraction of the right ventricle, blood is ejected across the pulmonary semilunar valve into the main pulmonary artery and then into the lungs, where carbon dioxide is exchanged for oxygen across the alveolar-capillary membrane.

Oxygenated blood then returns into the left atrium through the four pulmonary veins. During ventricular diastole, the blood flows into the left ventricle across the open mitral valve. When the left ventricle contracts, the blood is ejected into the aorta through the aortic valve; then is delivered to the various organs, where oxygen and nutrients are exchanged for carbon dioxide.

The heart receives blood through the left and right coronary arteries. These are the first arterial branches of the aorta and originate in outpouchings of the aortic root called the sinuses of Valsalva.

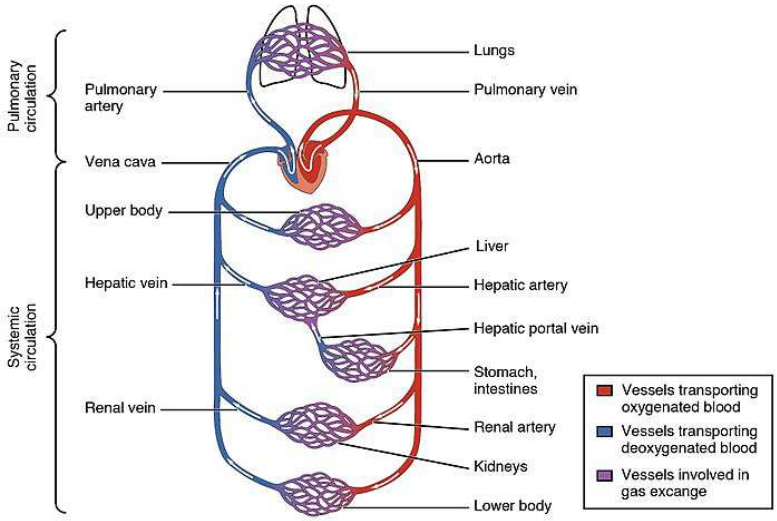

Figure 1.2: Circulatory system.

1.2 Biomechanical modelling of CS

It's possible to outline the cardiovascular system as in 1.3 , with a pump (the heart), a transport system (arteries), a collection system (veins), a distribution system (arterioles).

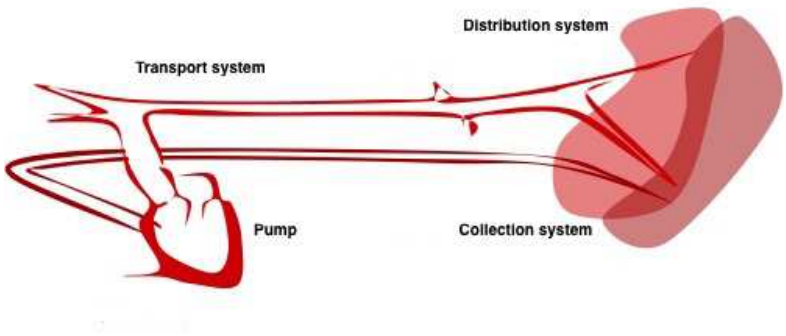

Figure 1.3: Schematic representation of cardiovascular system

The production of energy is linked with the forces generated by the cardiac muscle, the transport of energy is related with the elastic characteristics of vascular system, the dissipation energy depends on the viscosity of the fluid and on the geometric features of peripheral distribution network. There is an analogy between an electric circuit and the hydraulic behaviour of CS, in fact the CS can be represented by an electric circuit (Figure 1.4), where the pressure variation corresponds to a potential difference, the blood flow to a current and the vascular resistance to an electric one.

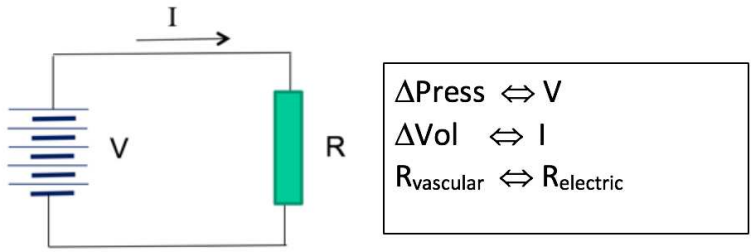

Figure 1.4: The electric circuit for SC, where the battery is the cardiac pump and the resistance is the vascular load.

1.2.1 The cardiac pump

In first approximation, from a mechanical point of view, the cardiac pump can be modelled by a continuous pump, that is a model of a pump which rotates with stable frequency and adjustable Ω; to this pump a system of flux regulation (S) is associated, like in fig 1.5.

In this model, the cardiac flow (that is the quantity of blood ejected in a minute) is constant and the flow is not pulsatile.

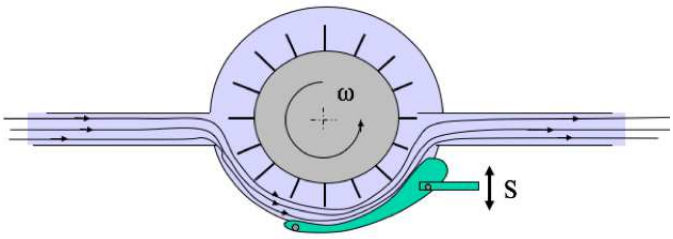

Figure 1.5: Pump's model with a constant flow.

In a more realistic approximation, the heart can be modelled by a pulsatile gen-

erator with a pulsatile flow and it's possible to simulate the elasticity of ventricular walls by an instantaneous regulation of the distance S (fig.1.6).

This parameter is called elastance and it's defined like the ratio between the pressure change in an elastic chamber and the corresponding volume change:

$$E = \frac{\Delta P}{\Delta V} \tag{1.1}$$

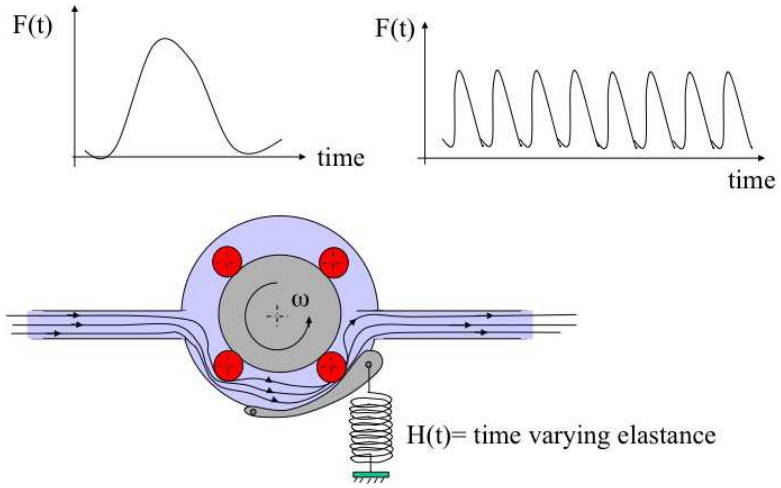

Figure 1.6: Pump's model with a pulsatile flow generator.

Considering a peristaltic pump, like in fig. 1.7, that takes the liquid from a reservoir and ejects it from an opening placed at a heigh h with a certain pressure $\rho \cdot g \cdot h$. This pressure can be considered as the ventricular pressure during systole to eject blood against an afterload h.

Plotting the relation between the flow and h, it's possible to obtain the Pressure-Flow curve in fig.1.8(a), characterized by a linear trend, with the maximum pressure when the flow is zero and a maximum flow when the pressure is zero. Every

point of the straight line is a working point of the pump with a certain pressure and flow.

There are two ways to modify the P-Q curve (fig. 1.8(b)). The first one is to varying the rotation velocity ω; with the increase of $\omega = 2\pi\nu$ the curve moves upwards and, as a consequence, also the maximum pressure and the maximum flow increase. The second way is to vary the distance between the rotation blades and the reservoir of the pump rotor (S), in this case for a constant value of the frequency, the curve is inclined, the pressure generated by the pump is increased and the maximum flow is unchanged.

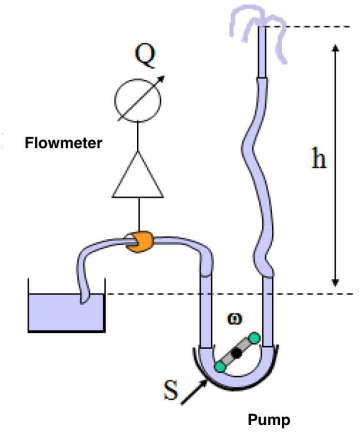

Figure 1.7: Peristaltic pump.

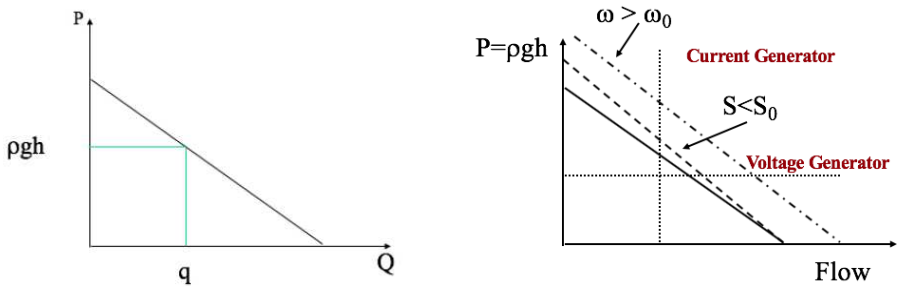

(a) Pression-Flow curve.

(b) Pression-Flow curve with variations of S and ω parameters.

Figure 1.8: Pressure-Flow relation.

The product between the pressure values and the flow values corresponds to the power that the pump transfers to the liquid and it has a bell shape in function of the flow (fig. 1.9).

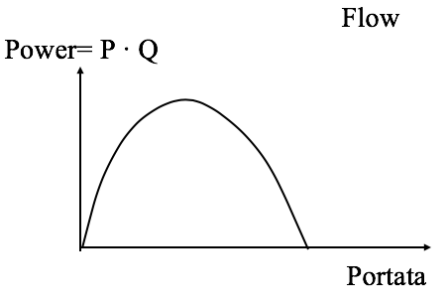

Figure 1.9: Power-Flow relation.

Considering the heart like a voltage generator with a high internal resistance,its load curve can be modified by acting on preload, contractility and cardiac frequency (fig.1.10).

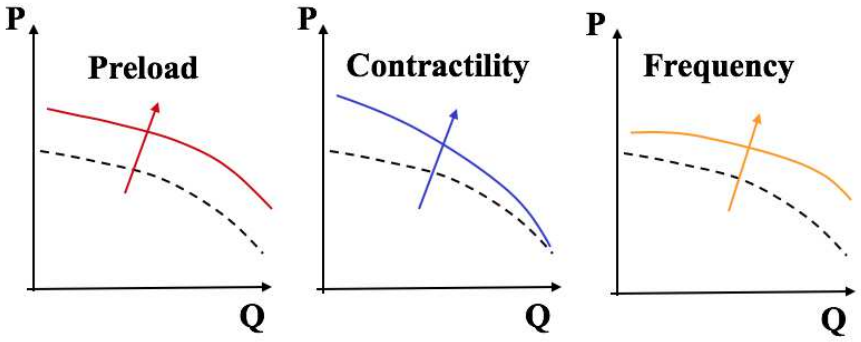

Figure 1.10: Pressure-Flow regulation

This mechanism was studied by Frank and Starling, in particular Frank studied, in a condition of constant flow, the pressure increasing generated by an increasing of preload, while Starling studied the increasing of the flow (in a constant pressure condition) during preload variation.

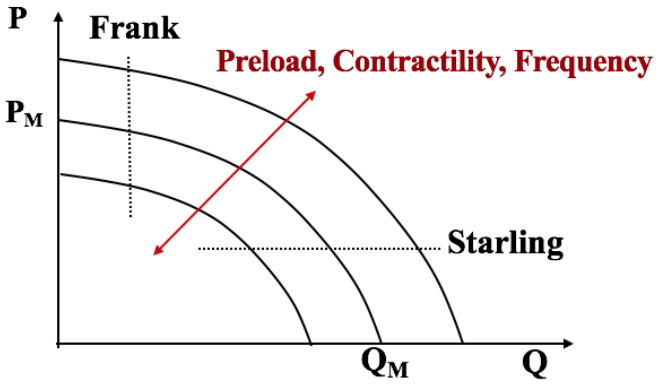

Figure 1.11: Frank-Starling mechanism.

In the fig.1.12 it's represented, for a healthy heart and a constant load (pressure), the trend of the cardiac output when the filling pressure varies: in a first phase the cardiac output increases in a directly proportional way with the filling pressure, then, by increasing a lot the filling (the ventricle is dilated), the curve is flattened; in this terminal phase, an increasing of ventricular filling determines a worst contractile performance.

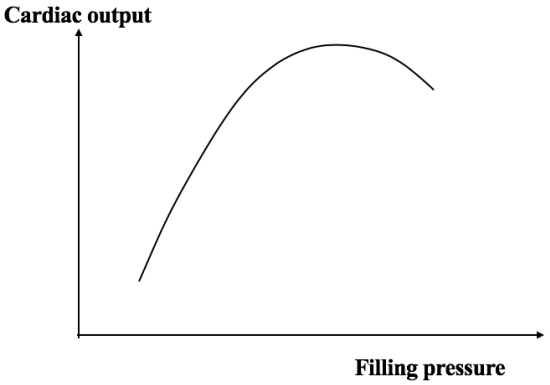

Figure 1.12: Relation between cardiac output and filling pressure in Frank-Starling mechanism.

1.2.2 The elastic characteristic of the ventricle

The mechanical behaviour of a ventricle is described by the Pressure- Volume loop (*PV loop*), that is a graphic of instantaneous pressure in function of ventricular instantaneous volume (fig. 1.13) The cycle can be divided into four basic phases: ventricular filling (phase a; diastole), isovolumetric contraction (phase b; systole), ejection (phase c; systole) and isovolumetric relaxation (phase d; diastole).

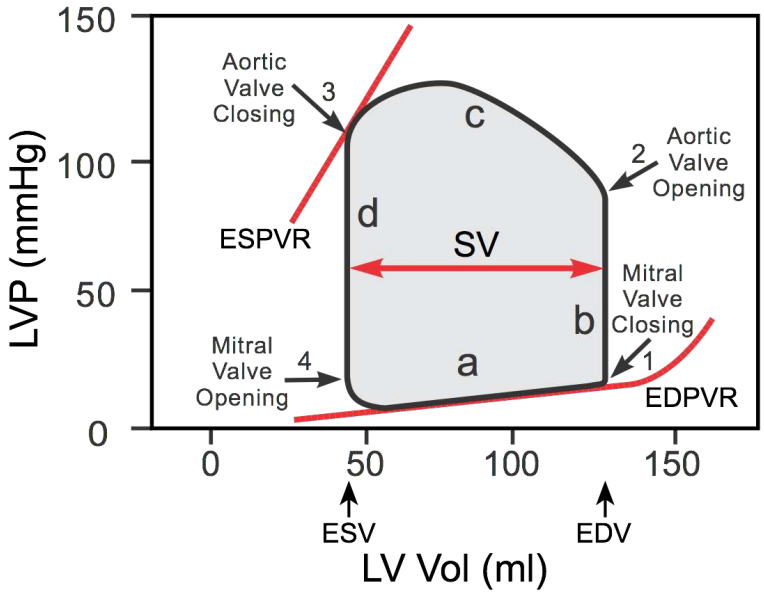

Figure 1.13: The PV loop diagram.

In phase 1, ventricle fills up (the venous blood passes from the atrium to the ventricle), the volume increases until it reaches a volume of end diastole, named telediastolic and the pressure varies because of the wall elasticity.

The phase 2 corresponds to the isovolumetric contraction, the mitral valve closes and the pressure increases rapidly until the aortic valve opens: in the intermediate phase between the opening and the closing both valves are closed, the ventricular volume is constant, the mechanical work is not produced and the rapidity of pressure variation $\frac{dP}{dt}$ reaches its maximum; this value is a good index for the contractile capacity of the ventricle muscular structure and is used to evaluate the effect of drugs and therapies.

In phase 3 the the pump does work and is when ejection begins, the ventricle empties and continues to contract, so the systolic ventricular pressure exceeds the aortic one, the aortic valve opens and permits the blood passage from the ventricle to aorta; the ventricular volume decreases and reaches the value of the

end of systole, named telesystolic, that corresponds to the systolic residual blood.

The systole is finished and the diastole begins in phase 4 with the isovolumetric relaxation: the ventricle stops to contract, the active elastic tension is reduced and the ventricular pressure decreases rapidly, so the aortic pressure exceeds the ventricular one and the aortic valve closes. Also in this phase the volume is constant because both the aortic and mitral valve are closed and no work is done. When the ventricular pressure falls below left atrial pressure, the mitral valve opens and the ventricle begins to fill (phase 1).

The work done by the ventricle is the integral, calculated on the whole cycle, of the product between blood pressure P and the blood volume variation inside the ventricle V and is represented by the area subtended by the PV diagram ($W = \oint PdV$). This work is named ventricular Stroke Work.

It's possible to calculate the instantaneous ventricular elastance through the use of the PV diagram, but this is quite easy during diastolic phase (the passive pressure increasing during the filling is associated to the correspondent volume variation), while it's more difficult for the contraction phase. For example, during the isovolumetric contraction and relaxation phase, the volume doesn't change, while the pressure increases or decreases respectively, so the elastance, according to equation (1.1) is infinite. Another similar situation is during ventricular ejection phase, when the volume decreases and the elastance is negative. To prevent this problem and to have a reasonable value for elastance in every point of PV loop, it's possible to consider the straight line that connects the point considered with the point (P=0, V_0), where V_0 is the ventricular volume when the walls are completely relaxed. In this way, the elastance of a particular point in the cycle is represented by the slope of the straight line that connects it to (P=0, V_0) (fig. 1.15). This method can be applied to every point of the PV cycle to obtain the temporal curve

of ventricular elastance, fig. 1.14. In this figure it's evident that elastance is low during diastolic filling and high at the end of ejection: so the ventricular walls are rigid in systole when the cardiac muscle contracts and elastic in diastole, when the cardiac muscle relaxes. The highest value of elastance is reached at the end of systole, in fact this has been proposed as index of ventricle contractile function.

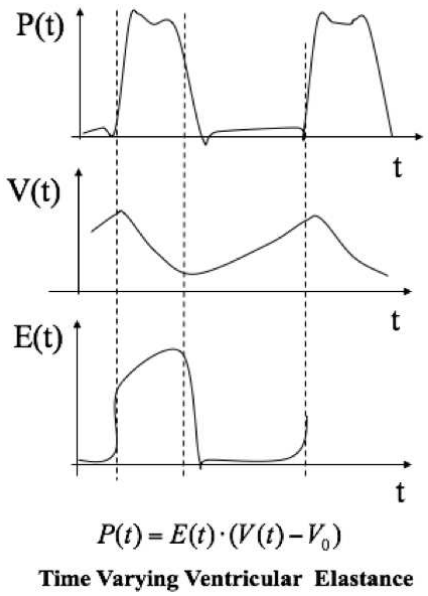

Figure 1.14: Pressure, Volume and Elastance trends during a complete cycle.

Because the P-V cycle is in function of time, the ventricular elastance can be expressed as a function of time too and every value of instantaneous pressure can be represented as product between elastance and volume:

$$P(t) = E(t) \cdot (V(t) - V_0) \tag{1.2}$$

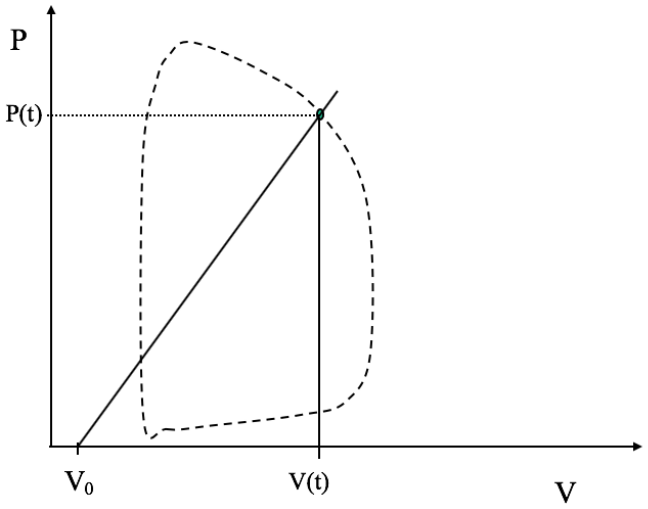

Figure 1.15: Representation of the elastance as the slope of the straight line that connects a point of the PV cycle to (P=0, V_0).

The PV loop cycle and, as a consequence, also the elastance curve in function of time, can be modified with the variation of preload, afterload and contractility parameters. The preload is defined as the initial lengthening of miocardic fibers before contraction, in the ventricle this is represented by the pressure at the end of diastole. The afterload is the sum of all resistances that oppose the contractile force, in the ventricle this corresponds to the aortic pressure that the ventricle has to exceed to empty.

With the variation of preload, constant afterload and contractility, the PV cycle is modified like in fig. 1.16 (a). When the preload increases, the volume of end diastole and the pressure of end systole increase. When the afterload is varied and the preload and contractility are constant, as in fig. 1.16 (b), the resistances that oppose the contractile force increase and the aortic pressure increases. With the variation of contractility only, as in fig.1.16 (c), the contraction force of the ventricle increases, so the pressure at end systole increases (the ventricle ejects a greater quantity of blood).

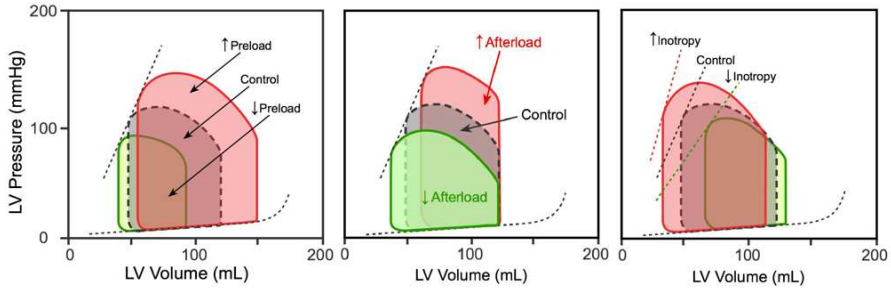

Figure 1.16: (a) represents the PV cycles when the preload varies; (b) represents the PV cycles when afterload varies; (c) represents the PV cycles when contractility varies.

It has been demonstrated (Suga and Sagawa) that, by altering the ventricle PV cycle with the variation of preload or afterload (without the variation of contractile function), the values of elastance at the end of systole are coincident. So the different PV cycles have the point of the end systole in a curve named *End Systolic Pressure Volume Relationship* that is almost straight, fig. 1.17 and fig. 1.18.

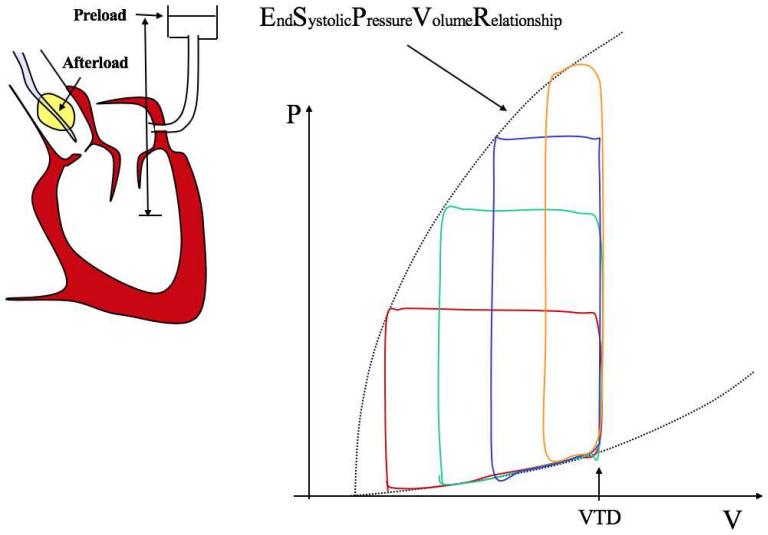

Figure 1.17: Variable afterload (R) and constant preload (VTD).

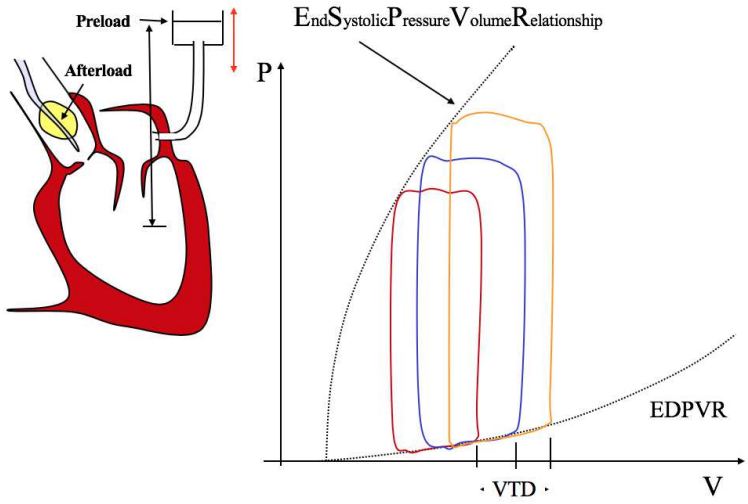

Figure 1.18: Variable preload and constant afterload.

The ESPVR is used as an evaluation, independent from the load, of the ventricular contractile function.

1.2.3 The arterial load

It's important to introduce the main concepts of Hagen- Poiseuille law to better understand the phenomena explained below. Liquids pass through conduits because there are some forces that act on them. For a real liquid a braking force exists between contiguous layers of liquid and it determines a laminar motion: the speed is not equal in every point of conduit section, but has a parabolic trend, the more peripheral layers move with a lower velocity than central layers. This is caused by the viscosity of the liquid that has two effect: one microscopic, that is to condition the speed between layers of liquid inside a conduit, and a macroscopic

effect, that is the pressure drop among the conduit that depends on flow, on liquid viscosity, on conduit length and on the radius fourth power.

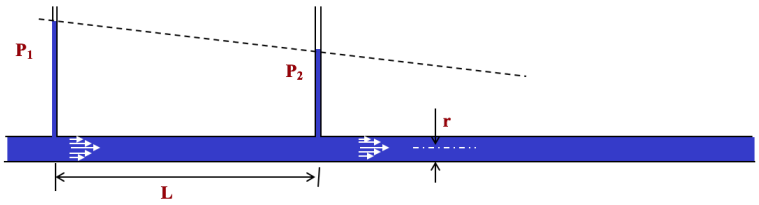

Figure 1.19: Fluid that moves inside a cylindrical conduit.

The expression of the flow in a conduit in terms of pressure drop and geometric characteristics (length L, radius r and viscosity η) represents the Hagen-Poiseuille law:

$$Q = \frac{P_1 - P_2}{R} = \frac{\pi}{8}\frac{(P_1 - P_2)}{\eta L}r^4 \tag{1.3}$$

where R is the hydraulic resistance.

Aorta and the big principal arteries have a big radius and their hydraulic resistance can be considered negligible, so the pressure drop is minimum for the same cardiac output. The mean cardiac pressure is unchanged at the entrance of arterioles, that regulate the blood supply of different organs. Arterioles have a small radius and a large hydraulic resistance, so the pressure drop is high and the flow is limited. For the Hagen Poiseuille law, the hydraulic resistance depends from the inverse of the radius fourth power, so small radius variations are sufficient to determine large variations of resistance and flow. Arterioles, capillaries and venules are fed by a unique source that origins from the aorta and this system is represented

in fig. 1.20. In correspondence of the cardiac pump outlet it's possible to consider a total hydraulic resistance and to not consider every single resistance of arterioles because the system is composed of many parallel vessels.

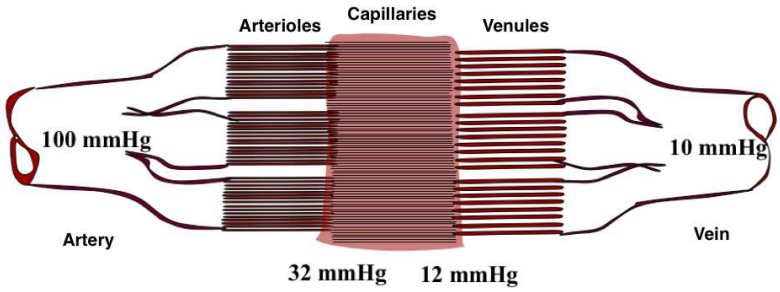

Figure 1.20: Blood vessels branching in CS: artery (aorta), arterioles, capillaries, venules and vein.

In a more realistic approximation, it's necessary to consider that aorta and other arteries in general are elastic so the arterial load can be represented as an elastic conduit that is able to deform and modify its volume when the blood passes inside it.

During ventricular systole, the cardiac pump exercises a pressure on the aorta elastic walls, that dilate until the restoring forces of the walls make up for internal pressure. According to Laplace law for cylindrical conduits: $\Delta P = \frac{\tau}{R}$, during systole phase the elastic tension increases and also the internal pressure. In this way, the cardiac pump, through the blood ejection that comes out from the ventricle at high pressure, transfers energy to the aorta; some of this energy is spent in vascular walls dilatation (PdV) and another part is used for blood passage ($\frac{1}{2}mv^2$).

During ventricular diastole, the artery empties the blood in excess in arterioles and comes back to the initial state of relaxation: the walls tension and the internal pressure decrease.

If the arterial walls are rigid, the energy transferred by the pump is used only to move the fluid, so in the same geometric conditions, for the same liquid and pressure, the blood moves more quickly in rigid conduits than in elastic conduits. Therefore the blood stored in aorta during systole phase is less; during diastole, when ventricular pressure stops the blood flow decreases considerably: the blood flow in this condition of rigid walls is not continuous. An elastic aorta permits to make more continuous the blood flow through the vessels.

After these considerations, it is possible to modelling the arterial system as a passive elastic load, formed by arteries (with resistance equal to zero) and arterioles with fixed hydraulic resistance (equal to the ratio between pressure and flow).

The parameter that describes the ability of an elastic structure to modify its volume, when the internal pressure varies, is called *compliance* and it's define as the inverse of the elastance parameter, so as the ratio between the volume variation and the pressure variation:

$$C = \frac{1}{E} = \frac{\Delta V}{\Delta P} \tag{1.4}$$

From the fig. 1.21(a) it's possible to note that the elastance has a non linear trend, but it depends from applied pressures. For low pressure there is a big deformation, so the vascular wall is very elastic (small value of elastance), but when pressure increases the walls become more stiffened until they are inextensible (large value of elastance). The elastic characteristic of the vessels feels the effect of physiological and pathological factors. For example in the case of a patient with a pathology that cause the loss of elastic condition, so the vessels stiffening, like the arterial hypertension, he has a different pressure pulse respect to a healthy patient, in the same condition of peripheral resistance and flow, so the same mean pressure (fig.1.21(b)). The elastance can be considered as the tangent in every

point of the curve, so it's more large in a hypertensive patient:

$$Elastance = tg\theta = \frac{\Delta P}{\Delta V} \tag{1.5}$$

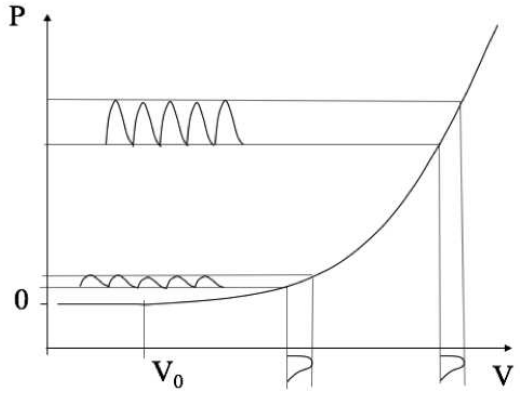

(a) Non-linear trend of arterial elastance.

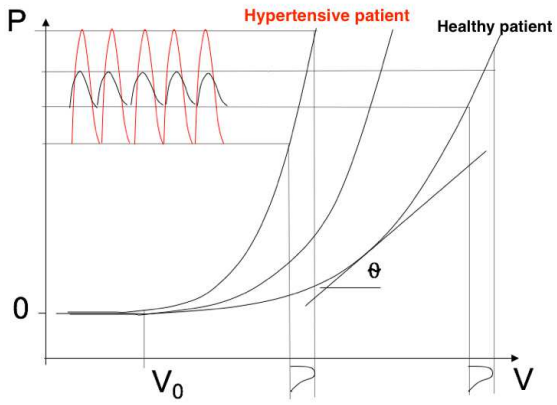

(b) Variations of elastance curve.

Figure 1.21: P-V arterial curves.

In fig. 1.22 is represented the aortic pressure curve: it reaches a maximum at about 130 *mmHg* during ventricular systole, in this point the pressure is called sys-

tolic; then, during diastole phase, the pressure decreases gradually until it reaches 80 *mmHg* approximately and this value is named diastolic pressure.

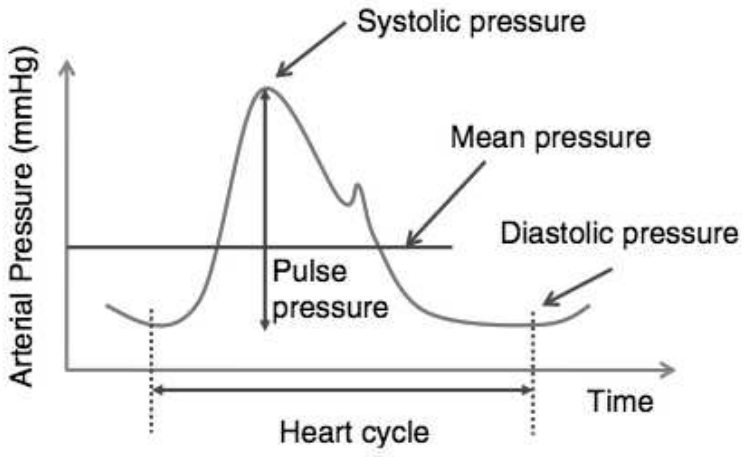

Figure 1.22: Arterial pressure trend during systole and diastole phases and pressure pulse representation.

The rapid pressure increasing when the blood is pushed from the left ventricle to the aorta is named pressure pulse and its amplitude decreased when the blood passes through the arteries. The pulse can be calculated as the difference between systolic pressure P_s and diastolic pressure P_d:

$$Pulse = P_s - P_d \tag{1.6}$$

In a healthy patient the pulse is about 50 *mmHg*. Because of the aortic pressure fluctuation between a maximum and minimum value, it's useful to consider a mean value to represent the arterial pressure; this can be determined with an integration of the arterial pressure curve between the start and the end time of the cardiac cycle and dividing this value by the cardiac cycle duration: this is equal to the calculus of the rectangle heigh equivalent to the trapezoids under the curve of the

arterial pressure:

$$Meanarterialpressure = P_{\mathrm{d}} + \frac{1}{3}(P_{\mathrm{s}} - P_{\mathrm{d}}) \tag{1.7}$$

1.2.4 Ventricle-artery mechanical matching

In the other section the models for the cardiac pump and the arteries are described separately, but it's possible to describe also the matching between them. A simple representation can be like the one in fig. 1.23, where the pump and the load are merely resistive elements.

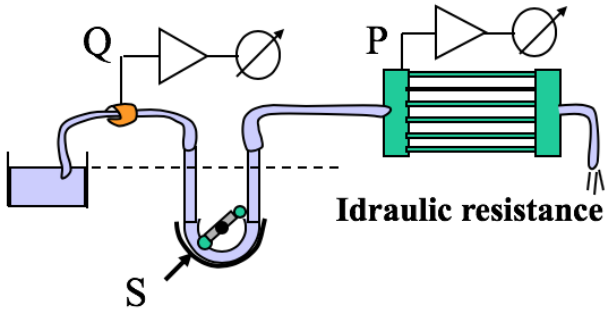

Figure 1.23: Simple mechanical matching ventricle-load

The 2 elements of the model have different characteristic pressure-flow curves (fig.1.24), the intersection between these two determines the working point of the system (fig.1.25).

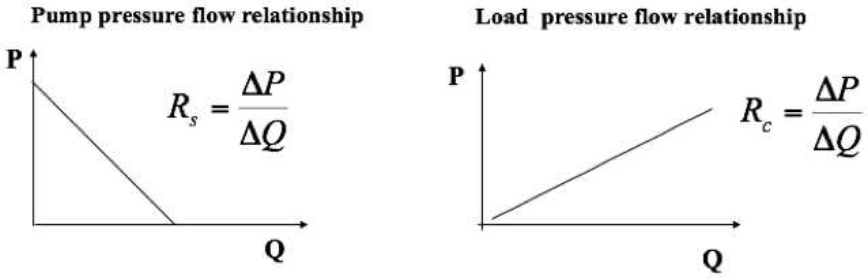

Figure 1.24: P-Q curves of pump and load

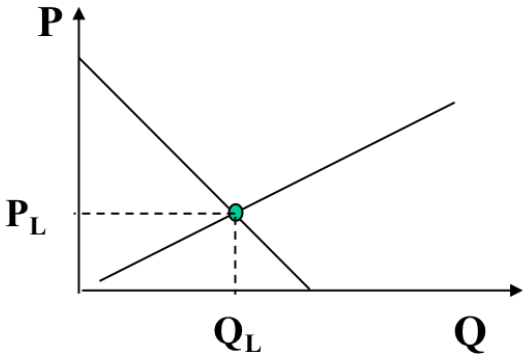

Figure 1.25: working point for simplified matching system.

It's possible to vary the hydraulic resistance of the load: in this case there are many different working point, one for every resistance; in the fig. 1.26 it's represented the transferred power for every work point that has a bell shape and it is evident that the maximum transfer is obtained when the internal resistance of the generator is equal to the resistance of the load.

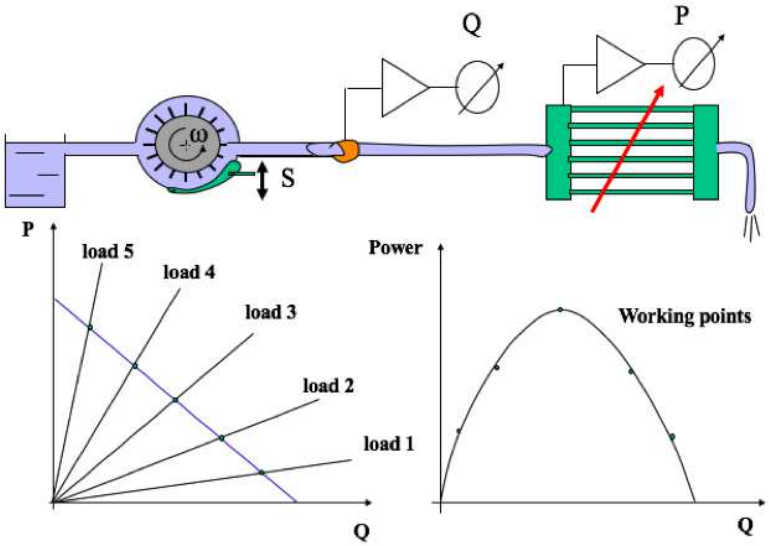

Figure 1.26: P-Q relation and Power-Q relation in the condition of variable load resistance.

There is the possibility to modify also the rotation velocity of the generator: in this case there are different parallel straight lines PQ, one for each frequency setted; also different curve of transferred power are obtained and the maximum is reached when the resistance of generator and the load are equal.

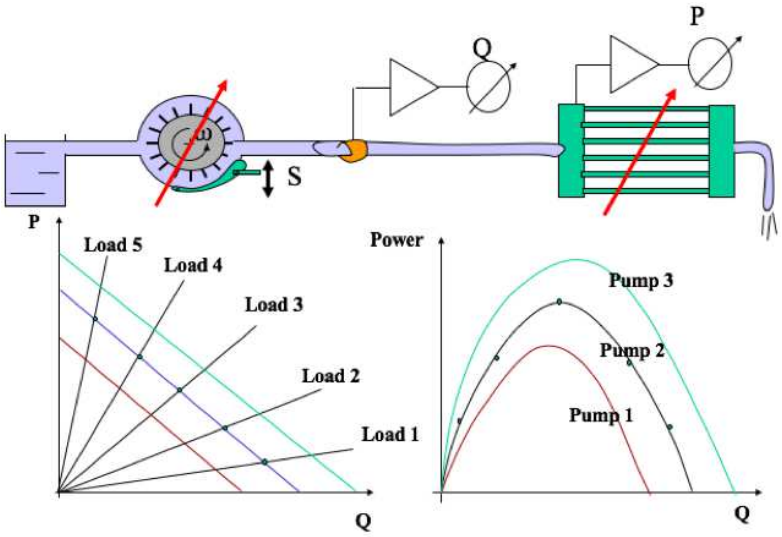

Figure 1.27: P-Q relation and Power-Q relation in the condition of variable resistance and variable rotation frequency.

A more realistic configuration is obtained when the elastic phenomenons are treated: the ventricle and the arteria are considered as elements with variable resistance. In fig.1.28) is represented this kind of model: a pulsatile flow generator with a non linear elastic behaviour E_v simulates the cardiac pump and is connected to a conduit with variable elastance E_a through the aortic valve; this conduit is connected also to a series of parallel conduits with hydraulic resistance $R_{\text{idraulic}} = \frac{8\eta L}{\pi r^4}$. Their total resistance is the peripheral resistance.

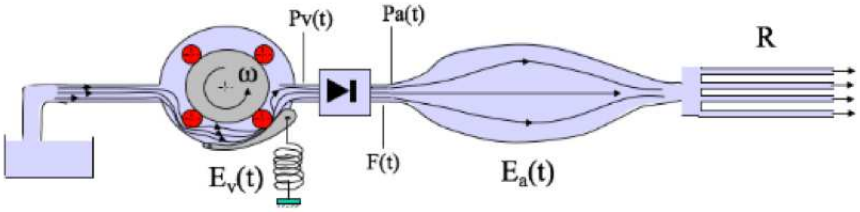

Figure 1.28: Model for the pump-load connection.

In fig. 1.29, the curves of pressure and flow for this model are represented: the green one is the ventricular pressure, the yellow one is the arterial pressure, while the black one is the flow. From this fig. 1.29 it's possible to note that:

- in the first phase, that is during systole, the arterial pressure and the ventricular pressure are superimposed until the valve is closed;
- then, when diastole begins, the ventricular pressure falls down and the arterial pressure remains at a positive value, it has a more dampened tread;
- the outflow from the cardiac valve increases during systole and it reaches a maximum value, but then it decreases and it reaches a zero value when the diastole begins.

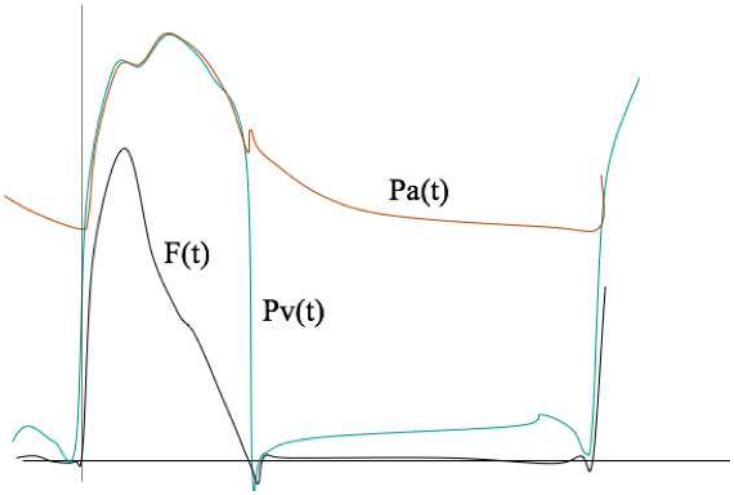

Figure 1.29: Ventricular, arterial pressures and flow curves for mechanical matching model generator and load with variable elastance.

1.2.5 The energetic transfer in ventricle-load matching

From an energetic point of view, the best matching, with the maximum transfer of energy, is obtained during systole (in this period the valve is open, so the ventricle and the artery are in communication),in fact in this phase the ventricular pressure and the arterial pressure are equal. The flow is given by:

$$I(t) = \frac{P(t)}{R} \tag{1.8}$$

where R is the peripheral resistance and P the pressure ($P_v = P_a$).

The continuity equation between pump and load is:

$$\Delta V_v = \Delta V_a + I(t)\Delta t \tag{1.9}$$

where ΔV_v is the ventricular volume variation and ΔV_a is the arterial volume variation.

By dividing both terms for ΔP:

$$\frac{\Delta V_v}{\Delta P_v} = \frac{\Delta V_a}{\Delta P_a} + F(t) \cdot \frac{\Delta t}{\Delta P} \tag{1.10}$$

With the condition ($P_v = P_a$) in the equation(1.10):

$$\frac{1}{E(t)_v} = \frac{1}{E(t)_a} + \frac{P_a(t)}{R} \cdot \frac{1}{\frac{dp_a(t)}{dt}} \tag{1.11}$$

The equation (1.11) describes the instantaneous relation among the parameters that govern the energy transfer between the ventricle and the aorta in every clinic condition.

In the case of hypertension the aortic elastance increases and the flow doesn't vary: the energetic transfer is maintained by the increase of ventricular elastance.

In the condition of aortic dissection, the aortic elastance increases and the ventricle can't increase its elastance, so it's a low efficiency situation: to maintain the energetic transfer is necessary to reduce the vascular resistance and/or the derivative of aortic pressure. Generally, from a medical point of view, the therapy consists on the administration of beta- blocking medical products and vasodilator drugs.

In a cardiac insufficiency case the ventricular elastance decreases and if the aortic elastance decreases, the flow can remain constant; but, if the aortic elastance is constant or increases, the equation (1.11) is satisfied by an aortic pressure increase, a vascular resistance decrease or a reduction of the term $\frac{dp_a(t)}{dt}$.

In the condition of a pulmonary hypertension, the vascular resistances increase, also the arterial pressure,so the vascular elastance increase: to maintain the energetic transfer is necessary to increase the ventricular elastance. If this one can not increase and the vascular resistance can't decrease, the derivative term $\frac{dp_a(t)}{dt}$ or the arterial elastance have to decrease.

If we ignore the terms P_a, R and dP_a/dt, it's possible to make a simplification of equation (1.11) and to represent the matching between cardiac pump and vascular load like the condition in which the ventricle and arterial elastances are equal (fig. 1.30).

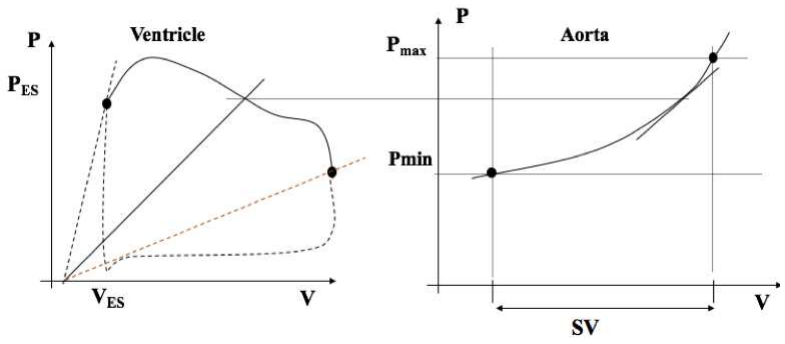

Figure 1.30: Ventricle-aorta matching

Chapter 2

The intra-aortic-balloon-pump

2.1 Active counterpulsation

Aortic counterpulsation (IABP) is the most commonly employed supporting technique in many cardiovascular critical condition, in fact it's widely used in patients with coronary disease and cardiac pump failure.

The studies about this method began in 1952 with experiments on animals conducted by Adrian and Arthur Kantrowitz and then in the 1960s years it was introduced in clinical practice especially in patients with cardiogenic shock.

This technique is based on rapid intra- aortic balloon (positioned in aorta) deflation, which reduces the ventricular afterload in systolic phase, followed by a rapid balloon inflation, which produces an increasing of diastolic pressure and , as a consequence, an improved coronary perfusion.

2.1.1 The IABP device

The IABP is composed of two principal parts: a mobile external console and an intraaortic catheter-balloon system, as in fig. 2.1.

The internal structure of catheter has two conduits, one for the gas passage

and one for the monitoring of arterial pressure in aorta, with a diameter from 7 and 9,5 French. As its distal extremity there is a balloon with a volume (from 25 to 50 mL) which has to be chosen in relation to patient height. In addition the balloon has a length from 17 to 27 cm. In 2008 a catheter with diameter of 7 Fr was introduced to limit the risks of ischaemia of the arm or leg perfused by the artery used for catheter introduction.

The external instrumental device is composed by:

- a monitor that shows the patient pressure and ECG signals in real time;
- an Helium (He) tank. Helium is inert gas, non explosive and with low molecular weight: it permits an easy balloon inflation and deflation and its chemical and physical characteristics limit the risk of air embolism in case of balloon break;
- a security disk, to separate the gas of the pumping system from gas running inside the catheter balloon;
- an electromechanical to control deflation and inflation timing according to patient cardiac events;

Figure 2.1: Standard IABP system.

A typical display of the device is showed in fig. 2.2, in which it's possible to see three important signals: the ECG signal, the arterial pressure and the balloon pressure waveform.

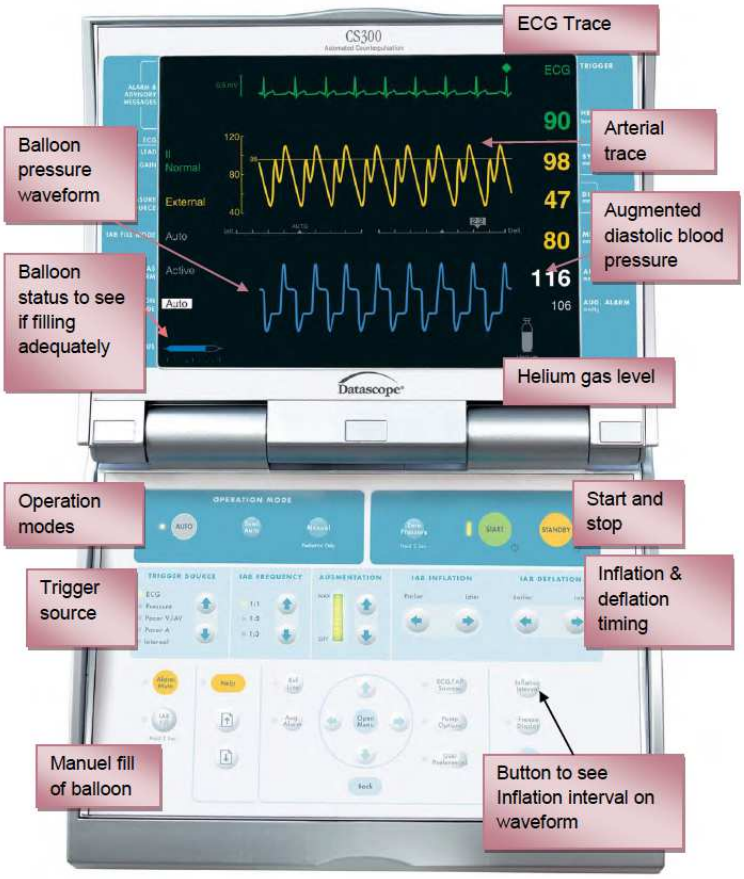

Figure 2.2: Display of Datascope device, model CS300 with the main parameters indicated.

The IABP is usually inserted percutaneously using the Seldinger technique, the catheter is inserted into patient femoral artery and then into the descending thoracic aorta, such that the balloon is 2-3 *cm* from the left subclavian artery and the proximal extremity is over the renal arteries. It can be inserted also in a surgical way: it's introduced in the vessel directly after this has been isolated medically.

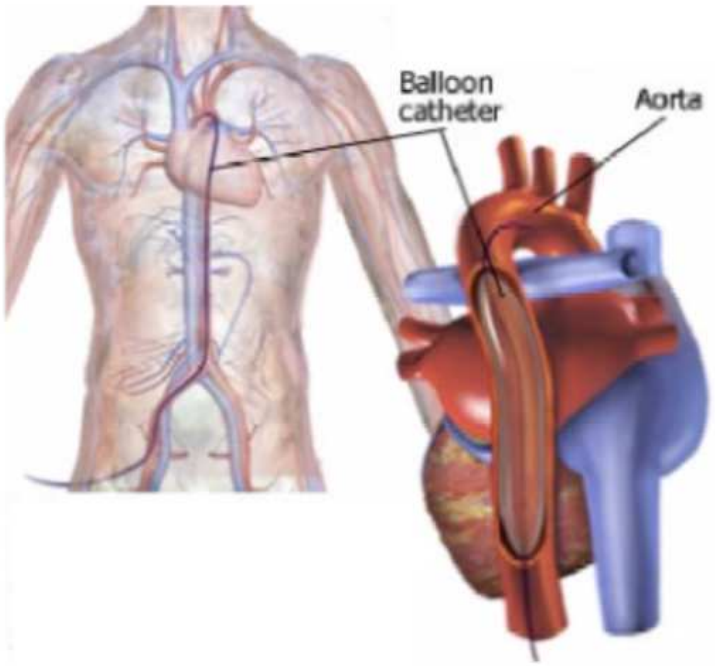

Figure 2.3: Correct insertion of catheter.

2.1.2 Triggering and timing

After the insertion, the catheter is automatically purged with helium, then the tip lumen is perfused with saline connected to a pressure transducer. In this way the aortic pressure signal is visible on the display and the operator can evaluate it.

To give the best haemodynamic benefits, the balloon has to inflate and deflate synchronously with the cardiac cycle ; for this a trigger is manually positioned on the ECG tracing by the operator. The most common trigger used is the ECG waveform, but the regulation acts with a delay of one beat, with possible problem in case of arrhythmia. To avoid this problem the control may be shifted to the arterial pressure signal but this solution requires a special catheter with a tip mounted pressure sensor, with an higher cost and not clear benefit.

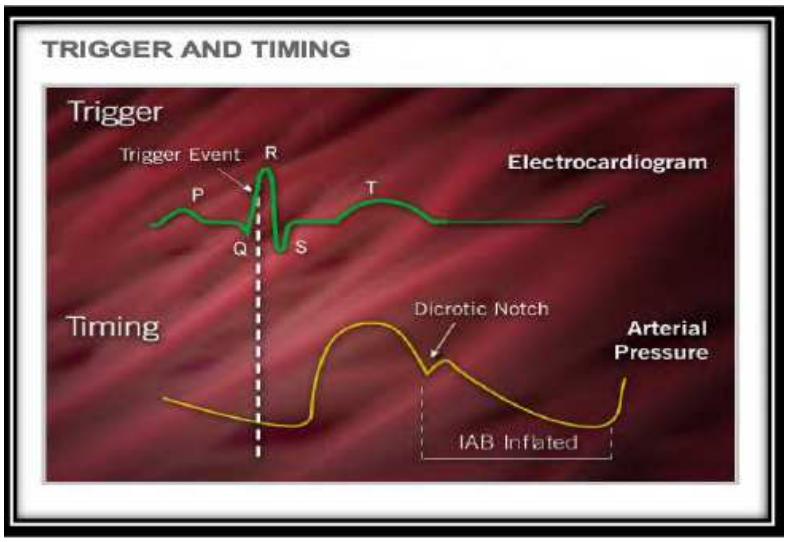

Figure 2.4: ECG waveform and arterial pressure signal used as trigger.

The balloon has to start to inflate at the onset of diastole, that corresponds to the middle of T wave on ECG waveform or to the dicrotic notch of the arterial pressure signal that is the aortic valve closure.

The balloon deflation has to begin at the onset of systole immediately before the aortic valve opening and this corresponds to the peak of the R-wave on ECG waveform.

Timing errors can produce improper inflation and deflation of the balloon, with negative physiological consequences. For example if the inflation is anticipated or the deflation is delayed, a potential premature closure of aortic valve may be produced, with increased left ventricular wall stress and oxygen consumption. Instead, a delayed inflation or an anticipated deflation, determines a lower increasing of diastolic pressure respect to that expected, with less benefits on coronary perfusion.

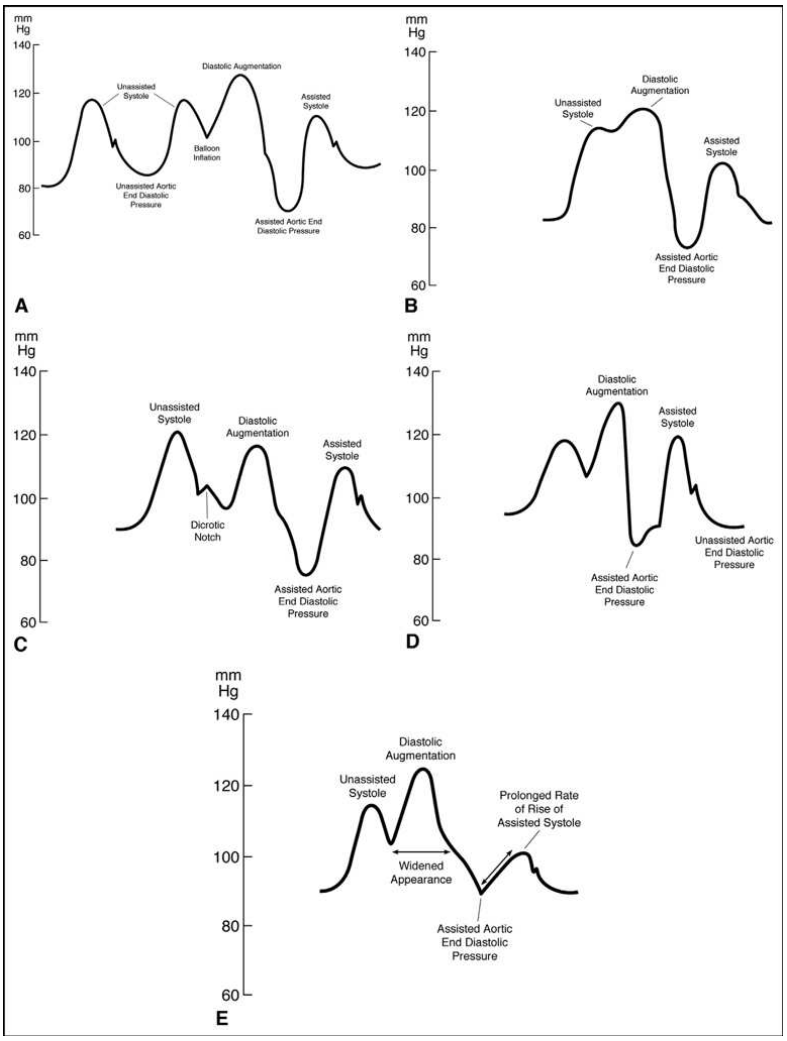

Figure 2.5: Timing errors. In A is represented the normal inflation and deflation IABP, with 1:2 frequency. In B is represented the earlier inflation, before the aortic valve closure. In C is represented the later inflation, after the diastole beginning. In D is represented the earlier deflation, before the end of diastole. In E is represented the later deflation, after the end of diastole.

It is also possible to set up the frequency ratio that refers to the augmented beats per cardiac cycle. Depending on patient's haemodynamic status, the balloon is programmed to assist every beat (1:1) or less, like 1:2 (one inflation every two cardiac cycles).

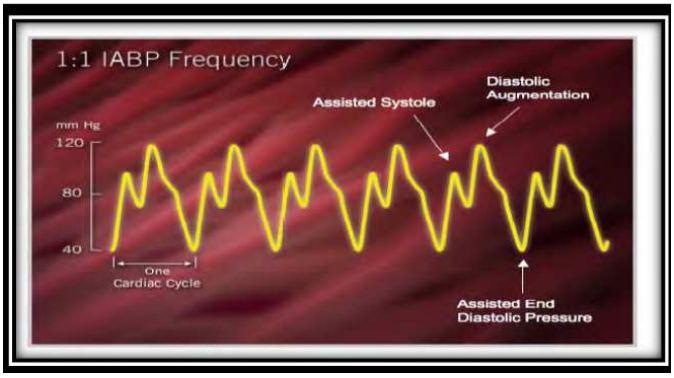

(a) waveform obtained with 1:1 frequency (balloon inflates every beat.)

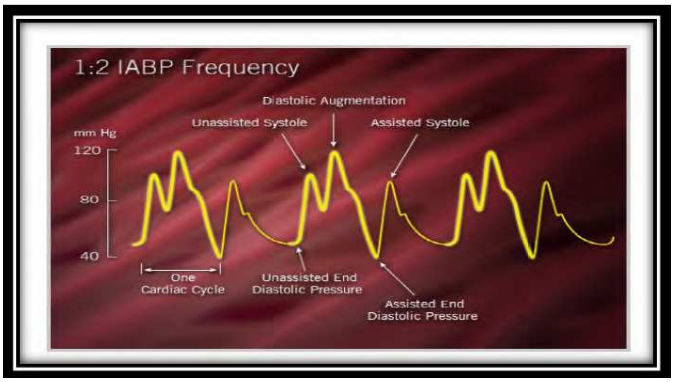

(b) waveform obtained with 1:2 frequency (balloon inflates every 2nd beat.

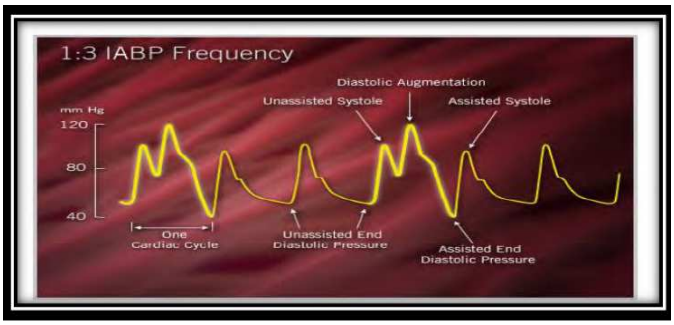

(c) waveform obtained with 1:1 frequency (balloon inflates every 3nd.

Figure 2.6: IABP waveforms.

2.1.3 IABP effects

From a physiological point of view the principal aim of IABP is to improve the myocardial function by with increasing myocardial oxygen supply and decreasing myocardial oxygen demand. In fig. 2.7 are represented the main effects of IABP in a schematic way.

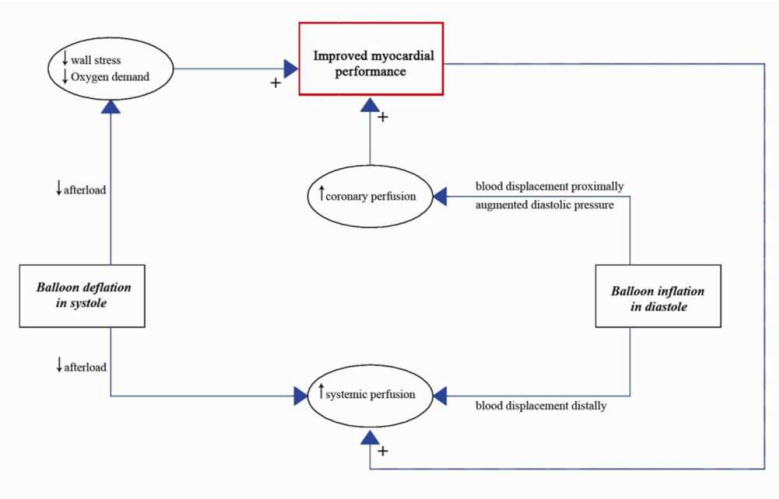

Figure 2.7: Physiological effects of IABP.

The balloon inflation at the onset of diastole permits to support the blood displace, this provides to increase coronary blood flow by increasing aortic diastolic pressure. With the balloon deflation at the onset of systole an afterload reduction occurs, so also the workload of the left ventricle and the myocardial oxygen consumption decrease.

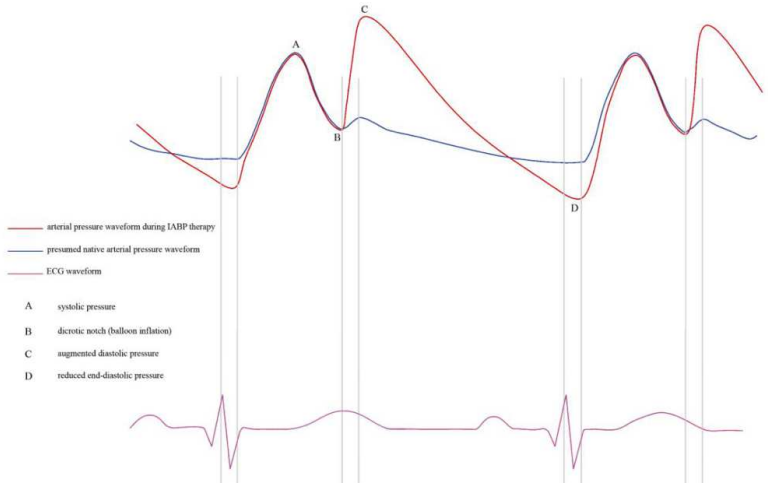

Figure 2.8: Arterial pressure changing with IABP.

From a biomechanical point of view the IABP function improves the matching between the cardiac pump and the load during systolic phase. In the first chapter it has been explained the best mechanical matching in energetic terms, that is when the elastance of the ventricle and the artery are comparable, but if the ventricular elastance decreases the equilibrium condition is broken and a worst mechanical system efficiency occurs. In this non- equilibrium condition, the IABP is able to adapt the ventricle elastance to the aorta during systole by the deflation of the balloon inside the artery. This makes easier the ventricular emptying and increases the Stroke Volume. In addition, the balloon inflation doesn't load the ventricle.

Aorta	↓systolic pressure, ↑diastolic pressure
Left ventricle	↓systolic pressure, ↓end-diastolic pressure, ↓volume, ↓wall tension
Heart	↓afterload, ↓preload, ↑cardiac output
Blood flow	↑→ coronary blood flow

Figure 2.9: Summary of haemodynamic effects of IABP therapy.

2.1.4 Complications and limitations

The Benchmark Counterpulsation Outcomes Registry published data of an experiment in about 1700 patient treated with IABP therapy between 1996 and 2000. From this data it was possible to note that major complications occurs on the 2,8 % of patients, so the method can be considered safety. It's important to underline that the common complications of IABP therapy are related to the presence of the catheter and the technique used for insertion. The rapid inflation and deflation of the balloon can cause some problems to the red blood cells and platelets, like anamia and thrombocytopenia. Other risks can be thrombus formation and subsequence embolization due to the device itself; that's why patients with IABP are usually treated with anticoagulant drugs, resulting in an increased risk of bleeding at the insertion site. There are many other complications like limb ischemia and the break of balloon (even if it's rare).

So in the most cases the results are positive and the procedure safety, but there are some problems that remain unsolved. One of this is the cost related to the device which requires a sophisticated pumping control; another problem is the efficacy of IABP in case of arrhythmias and the third main unsolved problem is related with the mechanical solicitation of arterial wall, that can cause problems to the patients. But there is a solution to this problems: it's possible to improve the ventricle-aorta matching with a passive solution without any time control.

2.2 Passive counterpulsation

Passive IABP is based on the same principles of the active one, but in this case the system exploits the pressure variations that, under correct conditions, are able to induce the balloon inflation and deflation without the use of energy coming from

the outside. In the passive IABP the balloon is not connected to an active pump and trigger, but to an external reservoir filled with Helium and the whole system is inflated with a pressure that is almost the mean aortic pressure. The removal of the ECG pressure controlled pump reduces the complexity and cost of the device and deletes the timing problems in case of arrhythmias.

During systolic phase, when the ventricle contracts, the aortic valve opens and the blood flows in aorta, the aortic pressure increases and it exceeds the mean value in the reservoir, so the balloon deflates in a passive way: the gas passes in the reservoir leaving space to blood that comes out from the ventricle and facilitates the ventricular emptying. In diastolic phase, the aortic pressure falls below the reservoir mean pressure value, so the gas flows from the reservoir to the balloon, this causes the balloon inflation and the arterial pressure is maintained higher in the coronary perfusion phase. Basically the balloon pulsation causes the increasing of diastolic pressure and the decreasing of systolic one, this results in a ventricular work reduction and a better coronary perfusion.

The passive counterpulsation is able to reduce the load elastance and to bring it closer to the ventricle reduced one. In passive counterpulsation no energy is supplied by external and the functional benefits are based on a more efficient management of the energy just produced by the ventricle.

There are also other indirect benefits. The pulsatile balloon reduces the amplitude of aortic pressure pulse, reducing the maximum pressure value and increasing the minimum one. The reduction of maximum pressure leads the decrease of ventricular wall tension, wall stress and the myocardial oxygen consumption. In this work it will be verify the pressure pulse reduction with the passive IABP and , because this is an important effect that consequent reduced mechanical wall pulsatility, which may improve also artificial endovascular prothesis insertion and attachment to the vessel walls.

The passive counterpulsation doesn't reduce the ventricular energetic production, at worst it doesn't produce any effects.

2.2.1 The effect on prothesis insertion

The vascular endoprothesis are artificial implantable devices which are inserted in vascular chambers to correct situations of possible danger (aortic dissection, arterial aneurysm rupture); these are manufactured with inextensible plastic material (dacron, teflon) eventually supported by a metallic stent with the function of maintaining an optimal shape also in the case of a highly irregular vessel. A main problem of these prothesis is the presence of endoleaks: connection between vascular lumen and the extra prosthetic chamber, which renders the therapeutic intervention inefficient in about 20% of cases.

This problem has two principal reasons:

- being the prothesis inextensible, also a little diameter difference determines an inefficient adaptation between prothesis and pulsating vascular wall;
- the pressure pulse is increased in the junction between normal and diseased vascular wall, due to impedance change and pulse reflection, with an increased pulsatility which makes more difficult to maintain a tight facing between prothesis tissue and vascular wall. This problem is further accentuated when, to dilate the prothesis and adapt its to the wall, a balloon is inflated inside and occludes the vessel. The aortic pressure widely increases (by a value that corresponds to the ratio between the cardiac output of the occluded vessel and the total one), with a dilation and a pulsatility increase in the junction point (the systolic pressure increases in the whole arterial system).

This is an emerging clinical problem and we decided to demonstrate how the mechanical vascular pulsatility can be reduced with passive intra- aortic balloon pump and how this may facilitate the adherence of the prothesis to the vessel's wall. This may allow to reduce the endoleaks and to limit the increase of the systolic arterial pressure during the prothesis positioning.

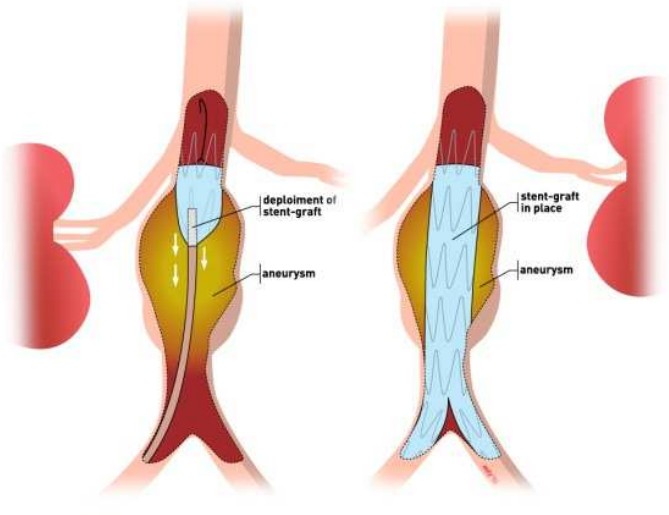

(a) Example of ptothesis insertion

(b) example of endoprothesis.

Figure 2.10: Endoprothesis example

Chapter 3

In vivo testing

This in vivo study has been a development of a previous work, but in this the aortic flow measurement is expected.

The passive counterpulsation system PIABP used for the functional validation on 10 patients in previous works and also in this work (with a new modified protocol), is represented in fig. 3.1. Using this system it's possible to switch from active to passive counterpulsation and vice versa through the rotation of a three ways stopcock inserted in the line connecting the balloon in the aorta. The device is composed by an Helium cylinder (A), a filling bag (B), a syringe that allows a controlled filling (C), a damping reservoir (D) connected to a manometer to verify the pressure, the switching stopcock (S) connected to the IABP control unit, to the intra-aortic balloon, to the ECG and to the aorta pressure transducer.

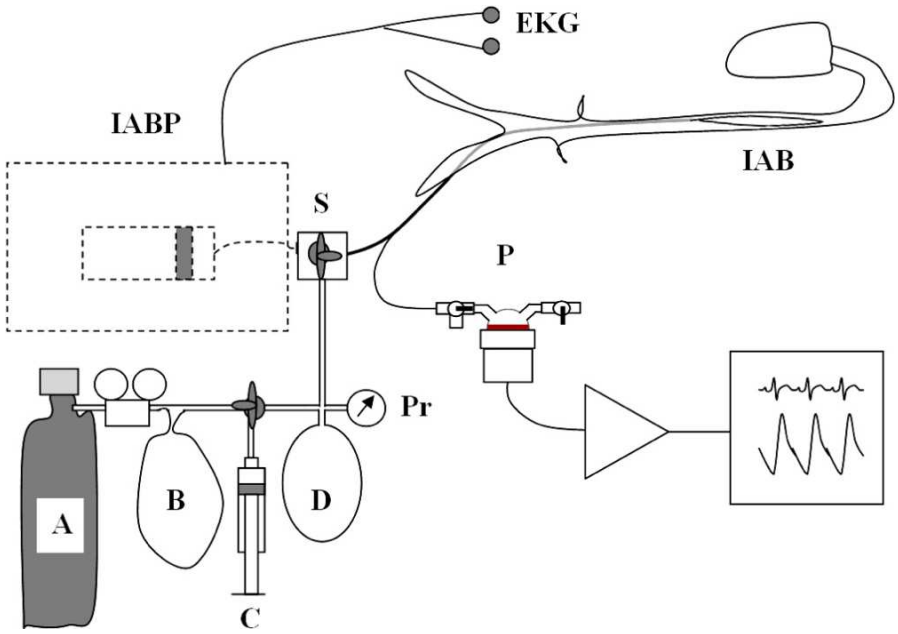

Figure 3.1: The passive counterpulsation device. A) is the Helium gas cylinder, B) is the filling bag, C)is the filling syringe, D) is the damping reservoir, Pr) is the reservoir pressure manometer, IABP) is the intra aortic active counterpulsator, EKG) corresponds to the electrocardiogram electrodes, P) is the aortic pressure transducer, S) is the active to passive stopcock switching, IAB) is the aortic balloon.

The counterpulsator analog output is interfaced to a Light Workstation (SparkBio, Bologna, Italy), that is an acquisition system of bioelectrical signals and it's able to operate the analogic to digital conversion of eight analogical signals that can vary in a range from -2,5 to +2,5 Volt, at 10 bits. This system leads to send the pressure and ECG signals to a connected PC by optic fiber way, with a resolution of 5 mV.

For the previous studies and for this work, other stopcocks A, B. C are inserted in the system to isolate every single component, that is the syringe, the filling bag and the dumping reservoir. In fig. 3.2 it's possible to see a schematic representation of the device used.

For this study the instruments that have been used are: the balloon (Datas-

cope) in polyurethane that is not extensible, with double lumen catheter used for active counterpulsation, an external reservoir formed by a bag for physiological solution with capacity of 1000 mL, a cylinder that contains 99% of Helium for medical use, with capacity of 5 l at 200 bar with a pressure reducer applied, the exit of the reducer is connected to the damping reservoir in soft PVC with capacity 2 l: in this the gas of the cylinder is placed.

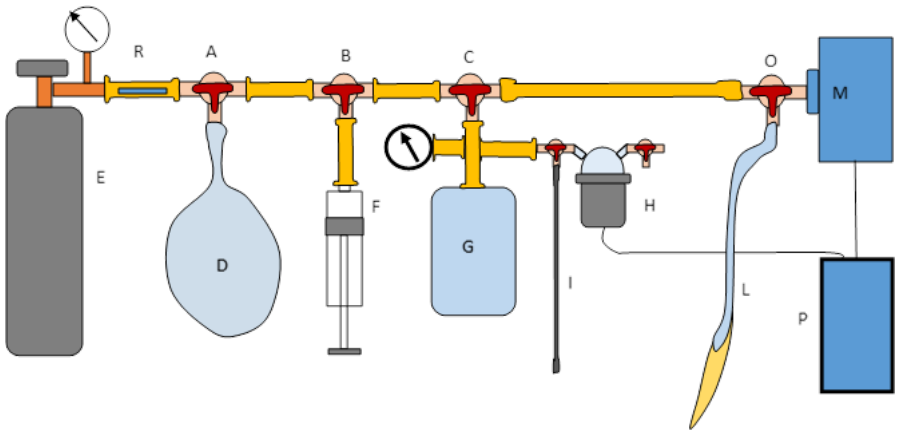

Figure 3.2: Passive IABP device used: E) Helium cylinder; D) Filling bag; F) Filling syringe; G) Dumping reservoir; A), B), C) stopcocks; H) pressure transducer; I) deflation line; L)IABP catheter; M) IABP counterpulsator; P) Light system.

The protocol for this work was approved by the Hospital ethical Committee with the condition of no additional trouble for patients treated but only conscious patients could be recruited and all of them signed an inform consent document.

This protocol envisaged:

1. to fill the passive counterpulsation system up to the stopcock O and repeat it more times but the gas cylinder has to be opened slowly;

2. To put on stand by the IAPB (*Datascope CS 300*) and to verify that the patient doesn't have problems without this device, to disconnect the catheter,

to insert the stopcock O between the counterpulsator and the catheter, to reconnect the counterpulsator and restart the standard counterpulsation.

3. To fill the damping reservoir D with Helium by rotating the stopcock A and opening the Helium cylinder slowly.

4. To measure the patient systemic pressure.

5. To aspire from the D reservoir with a syringe F and to fill the damping reservoir until the pressure is the patient diastolic pressure value.

6. To set up both the Light system for the acquisition of the aortic pressure and the ECG signal and the Doppler ultrasound (*Philips CX50*) registration.

7. To put in stand by the counterpulsation to be sure that the patient doesn't have problems.

8. To connected the passive counterpulsator to the patient by rotating the stopcock O (in this condition the aortic balloon is completely collapsed).

9. To inflate the balloon starting at the diastolic pressure step by step of 10 *mmHg* up to the systolic pressure and the same procedure has been repeated backward. For each step one minute signals have been registered. The data analysis included the systolic, the diastolic and the mean pressure for every step and the aortic flow measurement.

The protocol has been applied on 2 patients, but during the experimentation it's emerged an instrumental big problem. In fact, the pulse Doppler ultrasound signal to monitor the trans aortic valve blood flow (the most important parameter to be monitored) showed an unacceptable variability not only with different operators, but also for the same operator in the different steps of the protocol. It was sufficient to slightly change the ultrasonic beam orientation to have very different tracings

and it was practically impossible to have the same positioning in subsequent steps. On this evidence, the subsequent comparisons loose their value and we stopped the clinical protocol. We decided to shift the focus on bench simulation to demonstrate the effect of PIABP on pressure pulse amplitude and mechanical wall pulsatility during prothesis insertion.

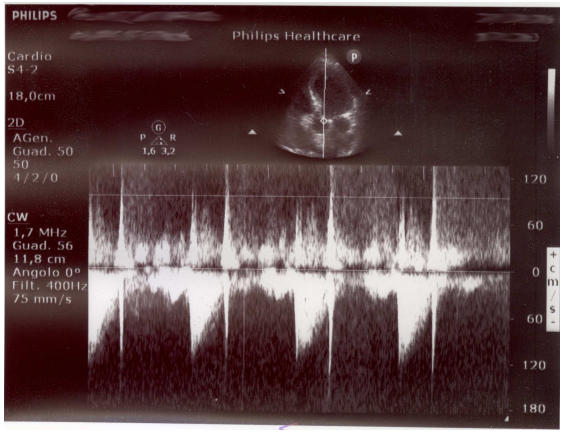

(a) Doppler Ultrasound signal for basal condition, P: 115/65 mmHg.

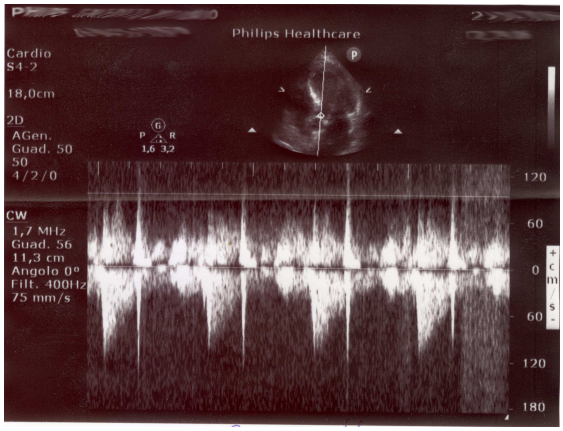

(b) Doppler Ultrasound signal with activated passive IABP at a 70 mmHg inflating pressure, P: 115/70 mmHg.

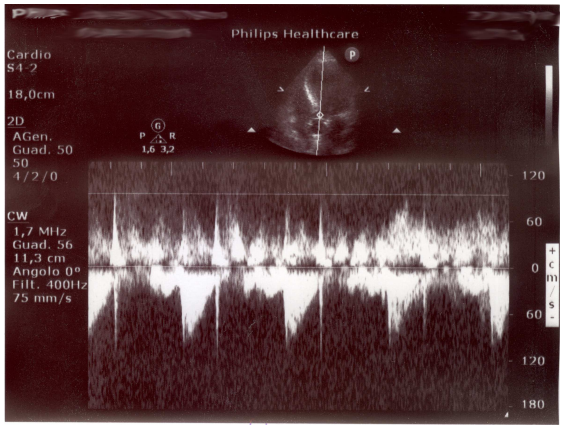

(c) Doppler Ultrasound signal with activated passive IABP at a 100 mmHg inflating pressure, P: 120/77 mmHg.

Figure 3.3: Doppler ultrasound signal registered for one patient in basal condition and in the case of the passive IABP activation.

Chapter 4

On bench simulation

As it has been introduced on the previous chapters, the validation on patients with the new modified protocol didn't give the result expected because of instrumental problems, very difficult to solve in a clinical setting, so the aim of this work has been focused on validation in the laboratory, with the construction and the use of a counterpulsator simulator to obtain quantitative observations on the effective reduction of aorta pressure pulse thanks to the use of the device. The pulsatility decrease is important also to support the adherence of prothesis on the vessel walls, in fact this is an unsolved recent clinical problem.

4.1 How to make a vascular model with defined biomechanical properties

In biomechanical cardiovascular simulations there is often the necessity to build mechanical components to mimic anatomical structures physiological behavior in basic and pathological conditions. It's possible to proceed in two ways:

- to make a mechanical model with biomechanical and structural acceptable

characteristics and to adapt it in a better way to mimic the physiological behaviour by the regulation of external parameters (vascular resistance, cardiac output, etc.); for example to have pressure curves with physiological values.

- To project the vascular structures starting from mechanical properties of the material (Young module) and adapting consequently the shape and dimensions, verifying the behavior experimentally. It's a more difficult methods than the first one, but it is mandatory when the model has to join functional and dimensional conditions to obtain structures with realistic behaviour and shape.

In this work the second method has been used to simulate two different aortas, one physiological and one stiffened, with dimensions suitable to evaluate the wall endoprothesis movement.

4.1.1 Aorta operative construction

For the aorta construction it has been decided to use a silicone material, because this can simulate the real properties of the vascular wall in a good way. As it has been said in the section above, two kinds of aorta have been used for this work: one that simulate a physiological condition and one stiffened (many pathological conditions cause the loss of vessels elasticity).

To implement the first one, it has been used one silicone tube, that was made for a previous work (Tesi Valentina Frangini, *Progettazione e realizzazione di un sistema di simulazione biomeccanico del ventricolo sinistro*) (fig. 4.1) and this can better reproduce the physiological elastic behaviour of aorta.

Figure 4.1: The white silicone tube that simulates the aorta in a normal condition.

For the stiffened aorta, instead, a new one has been made, using a transparent silicone that can simulate the condition of more rigidity of vascular walls; this kind of silicone *WACKER Elastosil 601 A* and its hardener *WACKER Elastosil 601 B* are shown in fig. 4.2(a) and 4.2(b).

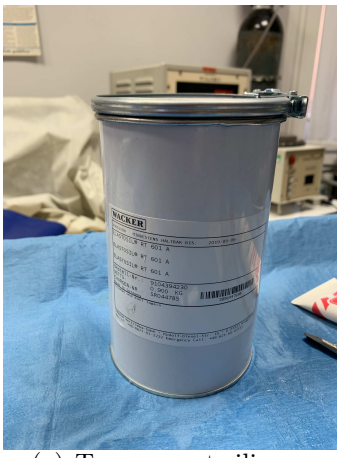

(a) Transparent silicone

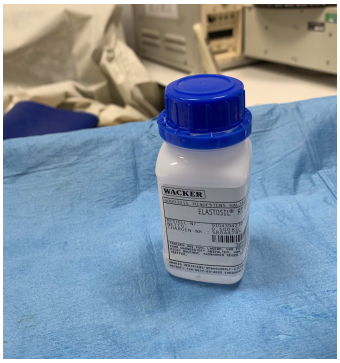

(b) Hardener

Figure 4.2: Transparent silicone and its hardener used for stiffened aorta simulation.

Then this transparent silicone has been smeared in a plastic plate (4.3(a)) and the result (after the material drying) is shown in fig.4.3(b). The final vessel obtained after all the steps is represented in fig. 4.3(c).

(a)

(b)

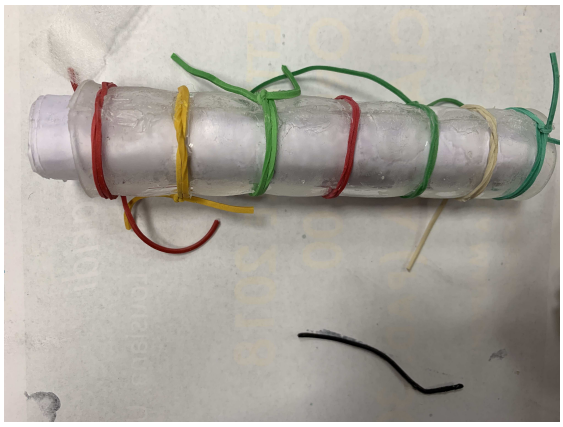

(c)

Figure 4.3: Steps to construct the stiffened aorta.

The two aortas volumes and diameters are indicated in the table 4.1, where for error associated to the diameters, the calibre sensitivity has been considered and the volume errors have been calculated with the error propagation method.

Aorta	**Diameter** cm	**Volume** mL
Normal	2,600 ± 0,005	37,2 ± 0,1
Stiffened	2,800 ± 0,005	58,8 ± 0,2

Table 4.1: The two aortas dimension.

4.1.2 Strain- Stress curve

After the two aortas realisation, the stiffness of these two vessels obtained has been evaluated.

The strain- stress curve of vascular walls has a typical elastomer trend, with a high strain (low Young module) for limited stresses and an increasing rigidity (high Young module) with strain increasing. This behaviour is due to the presence of elastin and collagen in the elastic wall molecular matrix. When the load is low the elastin interferes with a high strain; instead, when the load is higher the collagen interferes with a progressive stiffening of the structure and in this way the stress-strain curve modifies its slope.

For the strain-stress curve of two different silicones, an electromechanical system has been used to record the elongation variation in function of the load; this method permits to calculate the elastance.

A silicone strip is blocked between two terminals; then they are turned away with constant velocity. Through an experimental apparatus and a conversion system AD, it's possible to measure and acquire the elongations and the traction

forces applied to the sample.

The main components of the apparatus are:

- load cell (*Transducer C2G1-B* model),
- mechanical component,
- electric engine (*escap 26*),
- photodiode (*MCAB G8432*).

The load cell is used to convert the forces in electric signal directly proportional to the applied load (measuring range: (0,6- 3) kg; percentage accuracy: 0,02 %).

The mechanical part is composed by a screw of pitch 0,5 mm, that applies its motion to a sleigh. The screw presents four little wings perpendicular to its axis; one end of the sample is fixed to this through a terminal, while the other end is fixed to another terminal linked to the load cell.

The electric engine is connected to the screw and it gives to that a constant rotatory movement.

The photoelectric device allows the screw rotation revelation and it's formed by a photodiode that emits a light beam picked up by a transistor: the screw little wings interrupt periodically the beam and this permits the revelation of the screw movement, that is the elongation measurement.

In fig.4.4 it's represented a schematisation of the apparatus used to obtain the strain-stress curve of the samples considered.

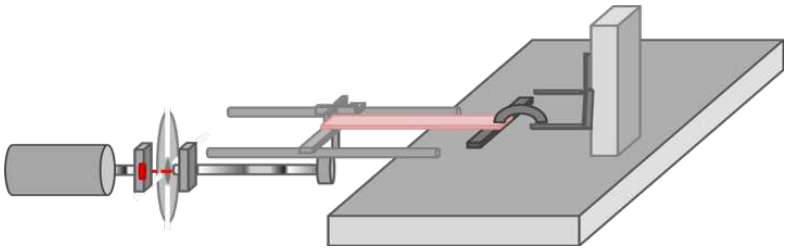

Figure 4.4: Schematic representation of the apparatus used.

In the next figures 4.5 and 4.6 the real adopted procedure is illustrated.

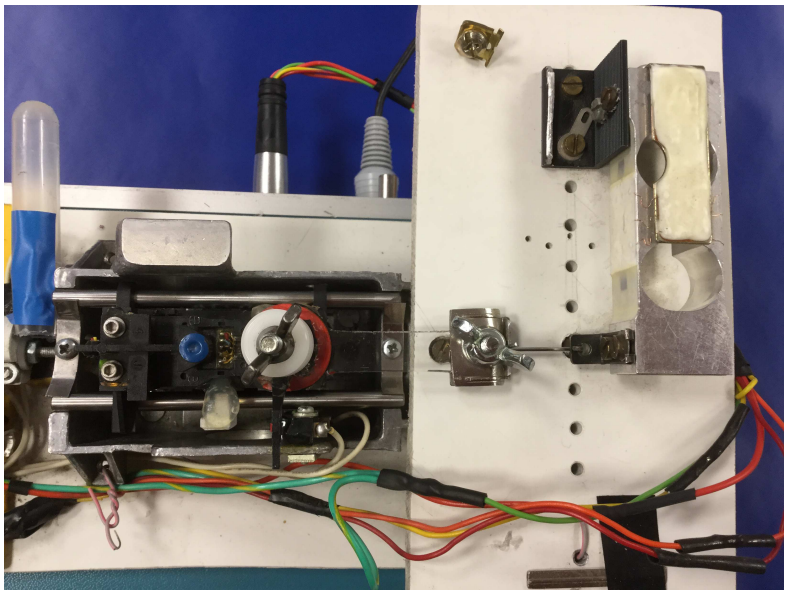

Figure 4.5: Sample fixed in the appropriate position.

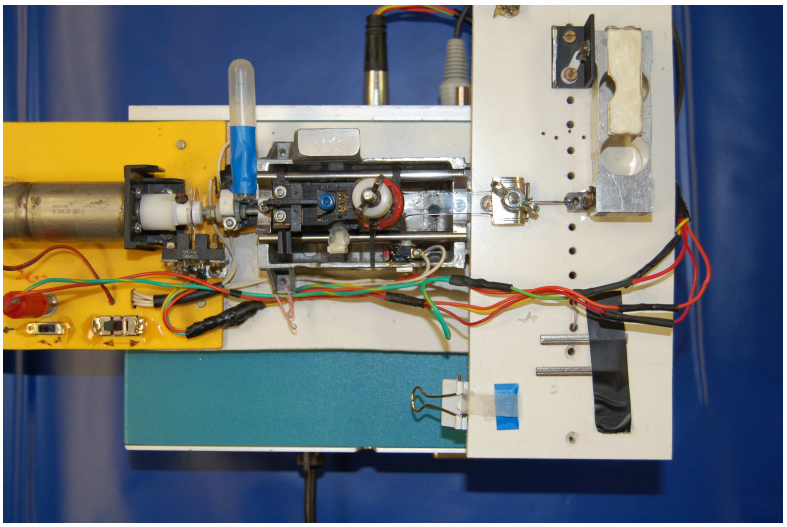

Figure 4.6: Sample elongation phase.

This apparatus is connected to the signal acquisition system ANSCovery with a voltage resolution of 2 mV; this allows to obtain the signal of the force applied (F) in function of the time (t) (Fig. 4.7).

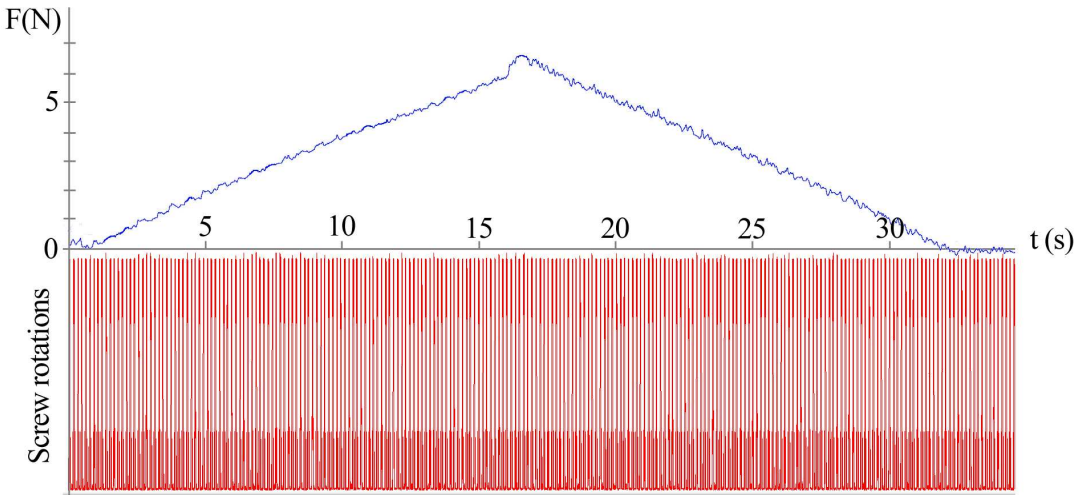

Figure 4.7: Signal displayed on ANSCovery: the blue curve is the force applied to the sample in function of time and it's composed by two parts, one for the risen (the elongation phase) and one for the fall (when the sample is returning to its normal length). The red signal represents the pulses generated by the transistor when the screw is rotating.

Basically, the quantity measured are the strain σ $[N/m^2]$ and the deformation (stress) ε, definable as:

$$\sigma = \frac{F}{A} \tag{4.1}$$

$$\varepsilon = \frac{l - l_0}{l_0} \tag{4.2}$$

where A is the section of the sample at rest, l_0 is the initial sample length and l is the sample length after the load has been applied.

Considering that every screw pitch corresponds to a sample elongation of 0,125 mm, after an opportune calibration, the graphs in fig. 4.8(a) and 4.8(b) have been obtained for the transparent silicone sample.

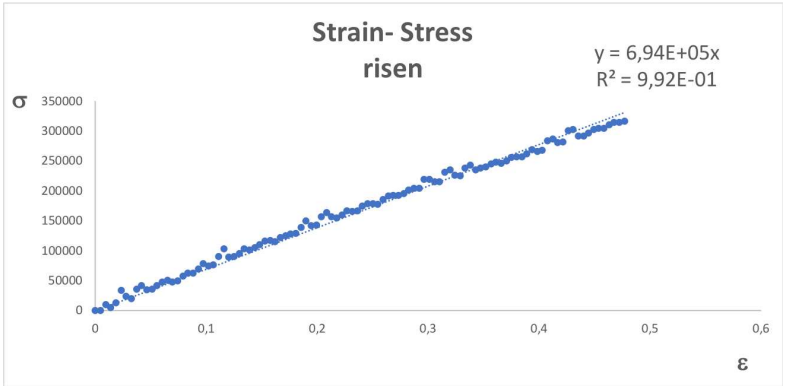

(a) Strain-Stress curve for transparent silicone sample during elongation phase.

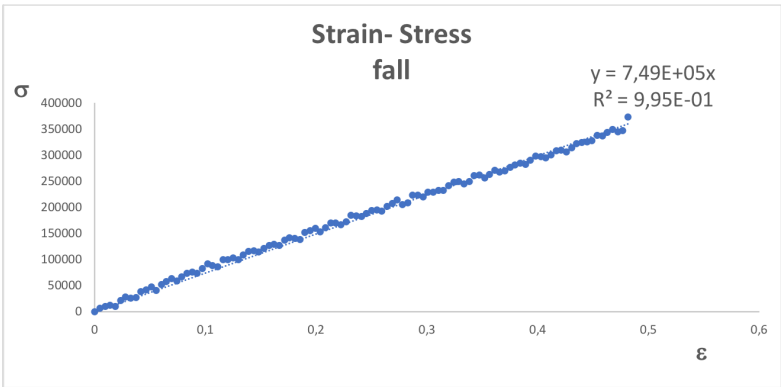

(b) Strain-Stress curve for transparent silicone sample when the sample is returning to its natural length.

Figure 4.8: Strain-Stress curve for transparent silicone sample.

The slope of the straight line is the Young module Y and it's possible to consider a mean value between its values during risen and fall phase, so : $Y = (7,21 \pm 0,02) \times 10^5\ N/m^2$, where the associated error is obtained by a regression method.

The same procedure has been repeated for the white silicone sample and the relative graphs of Strain- Stress relation are showed in fig. 4.9(a) and 4.9(b) .

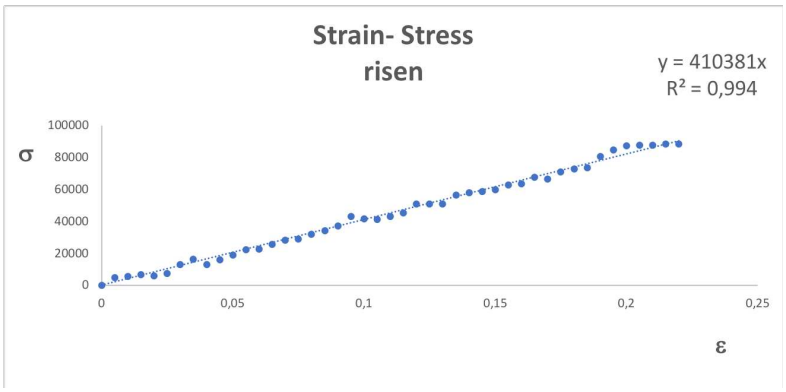

(a) Strain-Stress curve for white silicone sample during elongation phase.

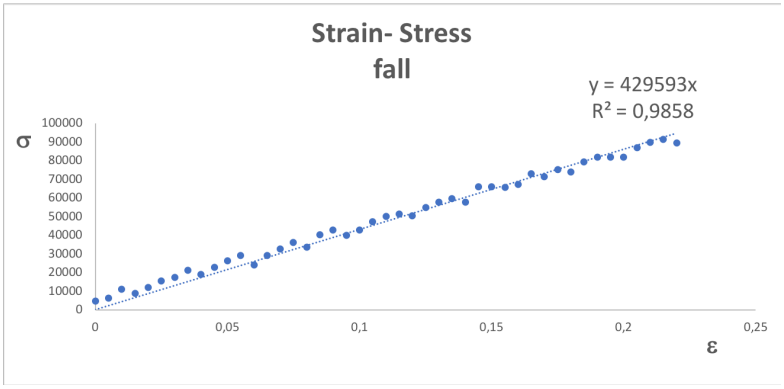

(b) Strain-Stress curve for white silicone sample when the sample is returning to its natural length.

Figure 4.9: Strain-Stress curve for white silicone sample.

In this case, the mean Young module Y with its associated error is: $Y = (4,2 \pm 0,03) \times 10^5\ N/m^2$.

Using this Young module and the Laplace's law (expressing the wall stress

as: $\sigma = \frac{P \cdot r}{2d}$), it's possible to calculate with an inflating pressure ranging from 80 *mmHg* to 120 *mmHg* a pulsation of 2 *mm* is expected for the normal aorta. For the stiffened aorta, with an inflating pressure ranging from 90 *mmHg* to 150 *mmHg* a pulsation of 1 *mm* is expected.

4.2 Materials and methods

The two aortas have been inserted in a cardiovascular simulation system (fig. 4.10) one at a time and inside them the passive counterpulsator has been inserted.

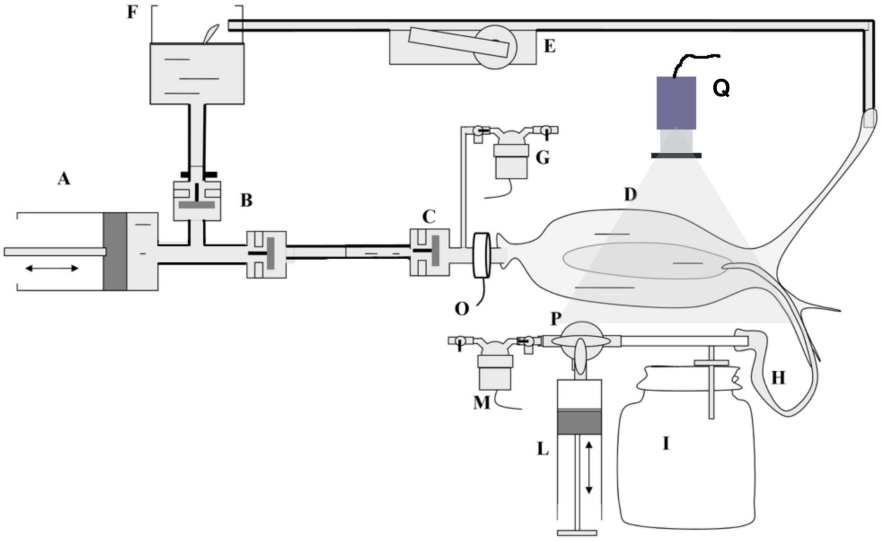

Figure 4.10: Passive IABP used for bench simulation: A) syringe pump simulating the ventricle; B) valves; C) aortic valve; D)aorta; E) vascular resistance; F)atrium; G)aortic pressure transducer;H)aortic balloon;I)damping reservoir; L) filling syringe; M)reservoir pressure transducer; O) flowmeter; P)stopcocks; Q)video acquisition camera.

For mechanical simulation of the cardiac action, it's usually used a pulsatile system, formed by a circular engine connected to a syringe that pumps water to the simulator (4.11). This pulsatile pump is also connected to an aorta and atria model through two unidirectional valves.

Figure 4.11: Pusatile flow generator.

The passive IABP used is formed by three main parts:

- a balloon that can inflate and deflate positioned in aorta;
- an external reservoir filled with air and connected to the balloon;
- a system for the pressure regulation;
- a system for the internal IABP pressure measuring.

It's possible to use the same balloon of standard IABP and the reservoir volume must be larger than that of the balloon to obtain sufficiently detectable balloon pulsations. The operating principle of inflation (during diastole) and deflation (during systole) is the same of the one explained in chapter 2. To vary the gas pressure, a syringe connected to the external reservoir was used: by inflating or deflating air inside the reservoir the pressure changes accordingly.

For the acquisition of pressure signals two transducers Baxter Edwards TruWave (fig.4.12) have been inserted in the system, one was positioned after the aortic valve and the other was connected to the PIAPB.

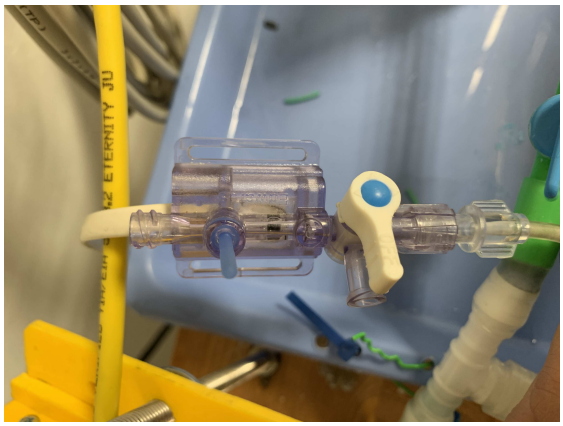

Figure 4.12: Example of Baxter Edwards TrueWave pressure transducer used.

These transducers have been inserted in the simulator through catheters and the other extremity was connected with an amplification and signal modulation circuit, then connected to the data collection system.

The flow signal has been collected by a flowmeter Biotrenex BL-610, positioned immediately after the aortic valve, in a way that permits to measure the incoming flow into the aorta. The flowmeter was then connected to the data recording system. Analog signals were sampled, digitally converted and stored by the ANSCovery System (Sparkbio Srl, Bologna, Italy).

Video recording during the experimentation was performed using a digital camera (model acA 1300- 75gc, Basler, Ahrensburg, Germany) interfaced with a Matrox Concord Card (Matrox, Dorval, Quebec, Canada) connected and synchronized to the ANSCovery System. Videos were acquired at a rate of 25fps and a frame dimension of 1280 $\times$ 1024 pixels.

Before the data acquisition, it was necessary to calibrate the pressure transducers by opening the stopcocks of these two, in this way it's possible to obtain the zero pressure, then it was sent a known pulse with corresponding value 100 mmHg and its amplitude was saved to give the reference value for the whole experiment.

Since the quantity of liquid ejected is constant, this has been used for the

calibration of the flowmeter.

The peripheral resistances have been regulated to simulate an hypertensive patient and a patient in a normal condition.

For both conditions an heart rate of 60 bpm was settled.

Measuring protocol

For each aorta the balloon pressure has been regulated beginning from a value lower than diastolic pressure until a value close to the systolic pressure step by step of 10 *mmHg*. For every condition, one minute of signal of interest (aortic pressure, aortic flow, PIABP chamber pressure) has been collected and also a corresponding video of pulsating aorta.

4.3 Data analysis

For every inflation condition:

- twenty pressure and twenty flow waveforms have been averaged and the systolic pressure, the diastolic pressure, the mean pressure and the mean pulse have been calculated through the ANSCovery software.
- Video frames corresponding to twenty beats have been extracted and for each beat the aortic volume has been calculated by a modified Simpson method (*A simple and innovative way to measure ventricular volume in a mechanical mock of the left ventricle*, Ivan Corazza, Lorenzo Casadei, Romano Zannoli). The volume curve obtained have been averaged, the maximum, the minimum volume and the difference between them have been calculated. In addition, also the maximum diameter, the minimum diameter and the difference between them have been calculated.

This analysis has been conducted for both the types of aorta.

4.3.1 Simpson method

To calculate the aortic volume variations with different balloon pressures inflation an image processing methods has been used (Simpson) (fig.4.13): if an elastic chamber is sliced, the total volume can be calculated as the sum of the volumes of all the slices. This method has been applied to the video registered by the camera during the simulation.

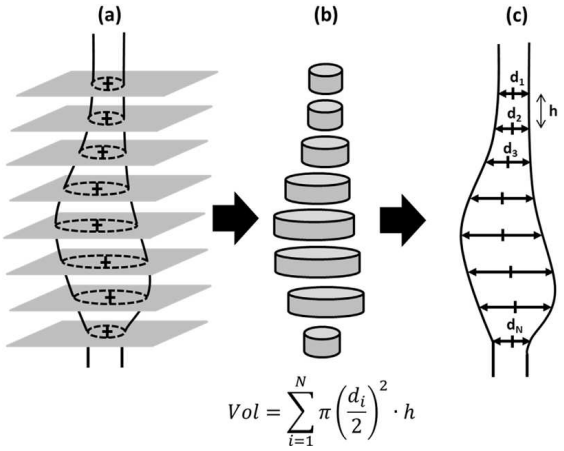

Figure 4.13: Methodology used for volume variations calculus: a)Generic chamber; b) cylindrical slices; c)diameter calculation by projection of the chamber on a reference plane.

The video acquired has been exported and opened in Matlab; in particular the software realized elaborates the data in this way:

- the video is divided in frames and every frame is saved in image format and is indexed;
- to optimize the elaboration time, the user has to choose a ROI in the first image and the same ROI is used for every frame;

- the image processing begins and it is based on the chromatic characteristic of the liquid or of the vessel (for the transparent aorta a blue inch is used to color the liquid, while for the normal aorta the white color is considered). In this way the blue white profile is extrapolated from the RGB image;
- a thresholding operation is done through the graythresh algorithm;
- the threshold BW image is corrected by the elimination of any isolated white spots through morphological operations;
- the shape is sliced along a vertical axis and each slice has a thickness of 1 pixel;
- the radius of each slice is calculated and also all the volumes;
- the slice volumes are summed;
- a digital signal is created representing the volume trend over time.
- since the volume of each chamber at rest is known, for calibration the volume can be calculated in mm of a single voxel (volumetric pixel).

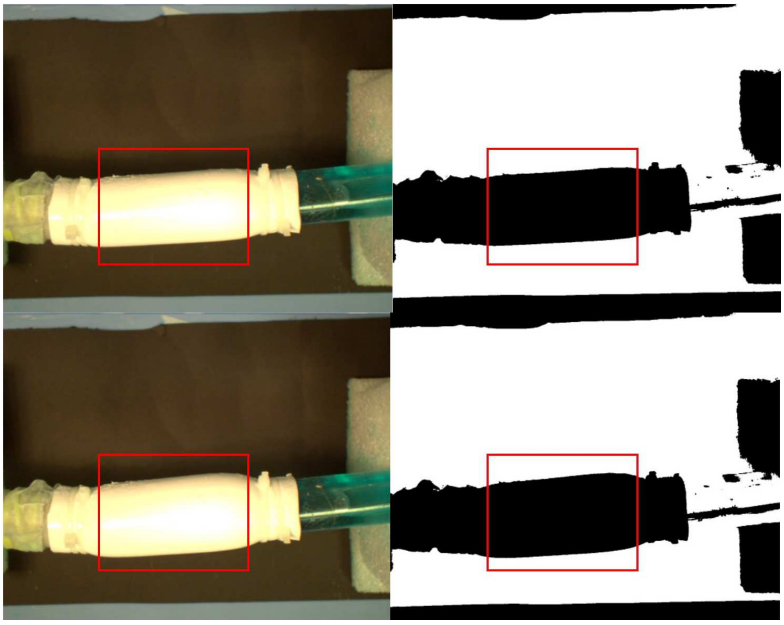

Figure 4.14: Frames extracted of the maximum and minimum diameter, with the selected ROI indicated and BW images obtained.

4.4 Results

Normal aorta

An example of the signals acquired of aortic pressure, balloon pressure and aortic flow (in the condition of 100 *mmHg* inflating pressure) is represented in fig. 4.15.

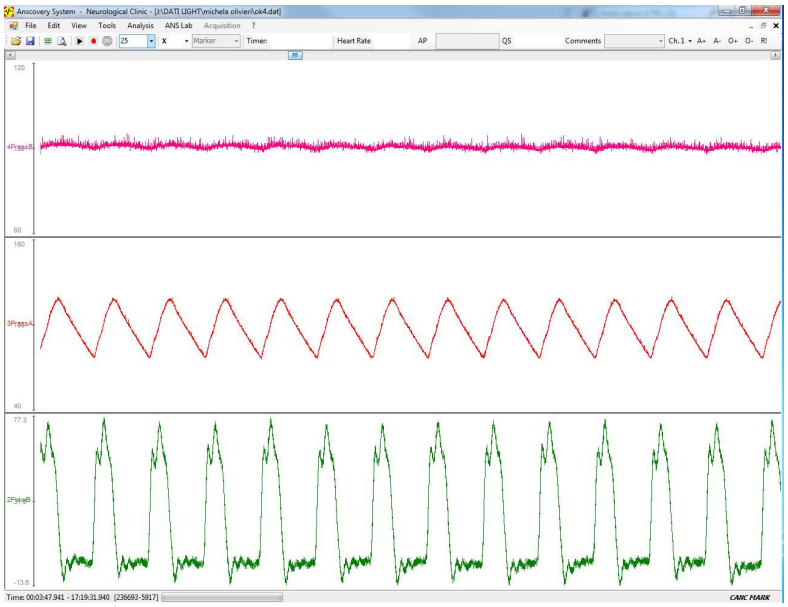

Figure 4.15: Example of balloon pressure, aortic pressure and aortic flow signals acquired with ANSCovery software in the condition of 100 *mmHg* inflating pressure.

The systolic pressure, the diastolic pressure, the mean pressure and the aortic pulse values are set out in the table 4.2.

Inflating pressure mmHg	**Systolic pressure±1** mmHg	**Diastolic pressure±1** mmHg	**Mean pressure±2** mmHg	**Aortic pulse±2** mmHg
0	121	78	92	43
60	119	77	91	42
70	119	78	92	41
80	117	77	90	40
90	115	80	92	35
100	115	82	93	33
110	115	85	95	30
120	116	87	97	29

Table 4.2: Values of systolic pressure, diastolic pressure, mean pressure and aortic pulse for each inflating pressure condition.

The graph obtained with these values is represented in fig. 4.16.

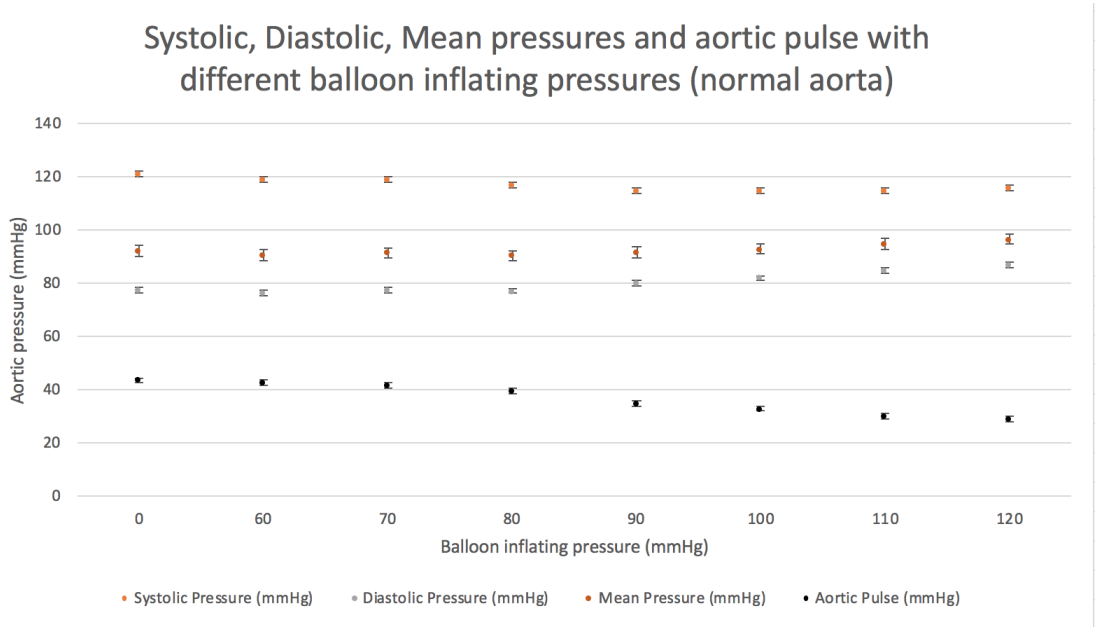

Figure 4.16: Systolic, diastolic, mean pressure trends with different inflating pressure conditions.

The mean complexes of pressure and flow obtained are represented in fig. 4.17 and 4.18.

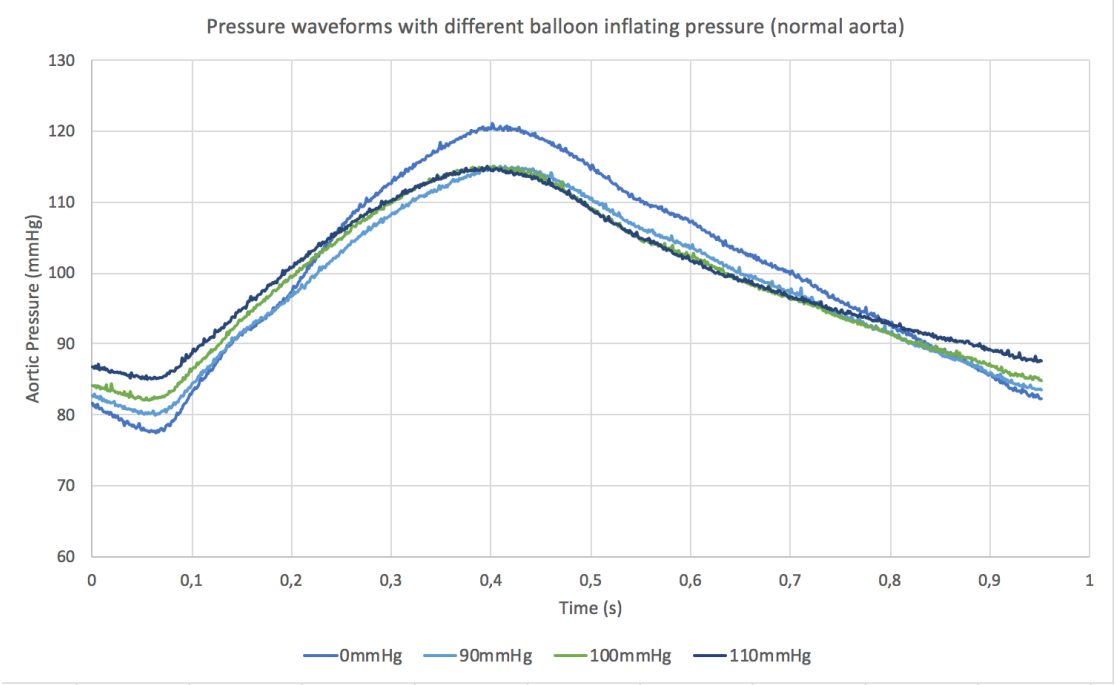

Figure 4.17: Pressure mean complexes in function of different balloon inflating pressures.

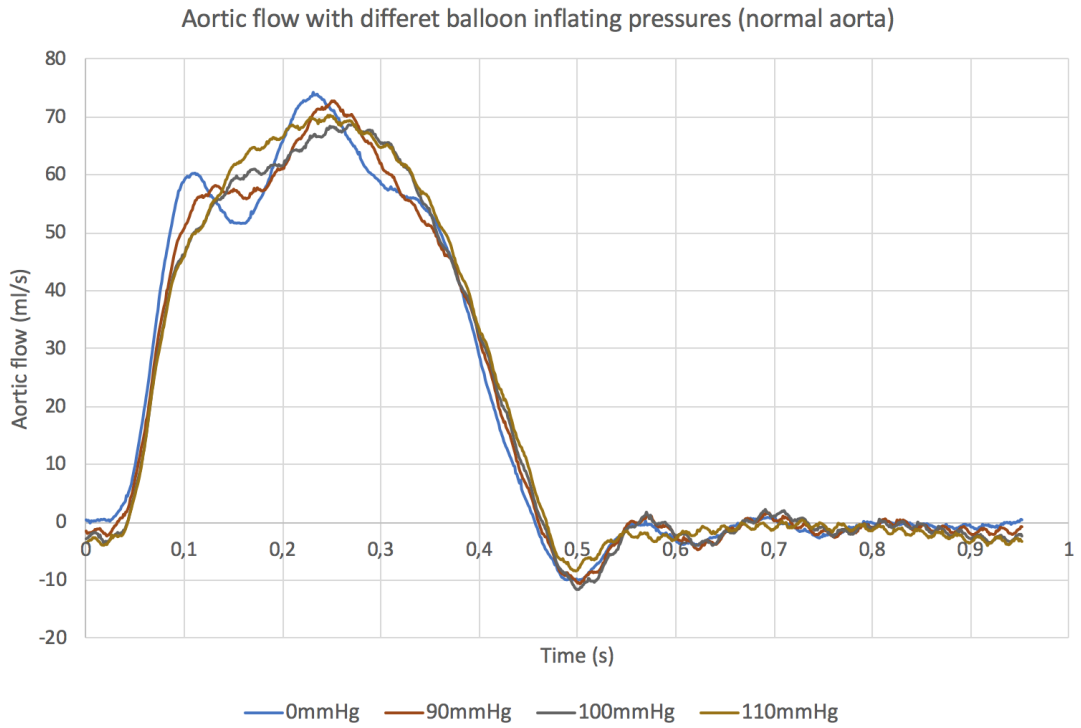

Figure 4.18: Flow mean complexes in function of different balloon inflating pressures.

The table 4.3 contains the maximum and minimum pressure values inside the PIABP.

Inflating pressure	**Max pressure±1**	**Min pressure±1**	**PIABP pulse ±2**
mmHg	mmHg	mmHg	mmHg
0	0	0	0
60	61	61	0
70	69	69	0
80	81	80	1
90	95	89	6
100	106	99	7
110	113	105	8
120	123	115	8

Table 4.3: Maximum and minimum pressure values inside the PIABP.

The volume values obtained for different balloon inflating pressure condition are presented in table 4.4.

Inflating pressure	**Vol max ± 0,1**	**Vol min ± 0,1**	**Δ Vol ± 0,2**
mmHg	mL	mL	mL
0	52,7	45,6	7,1
60	52,6	45,5	7,1
70	52,6	45,5	7,1
80	52,4	45,4	7,0
90	51,7	45,7	6,0
100	51,5	46,1	5,4
110	51,2	46,5	4,7
120	52,5	46,4	6,1

Table 4.4: Volume values obtained for every different inflating pressure condition.

The aortic volume graph for the values obtained is represented in fig. 4.19.

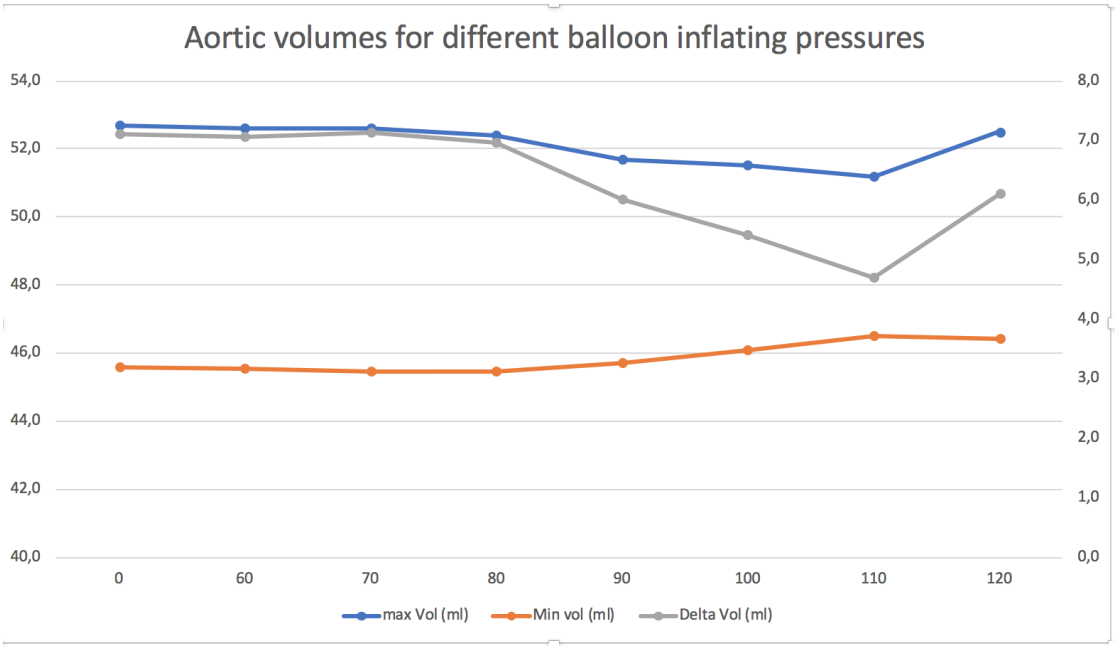

Figure 4.19: Aortic volume trend with different inflating pressures.

The mean complexes obtained for the aortic volume is represented in fig. 4.20.

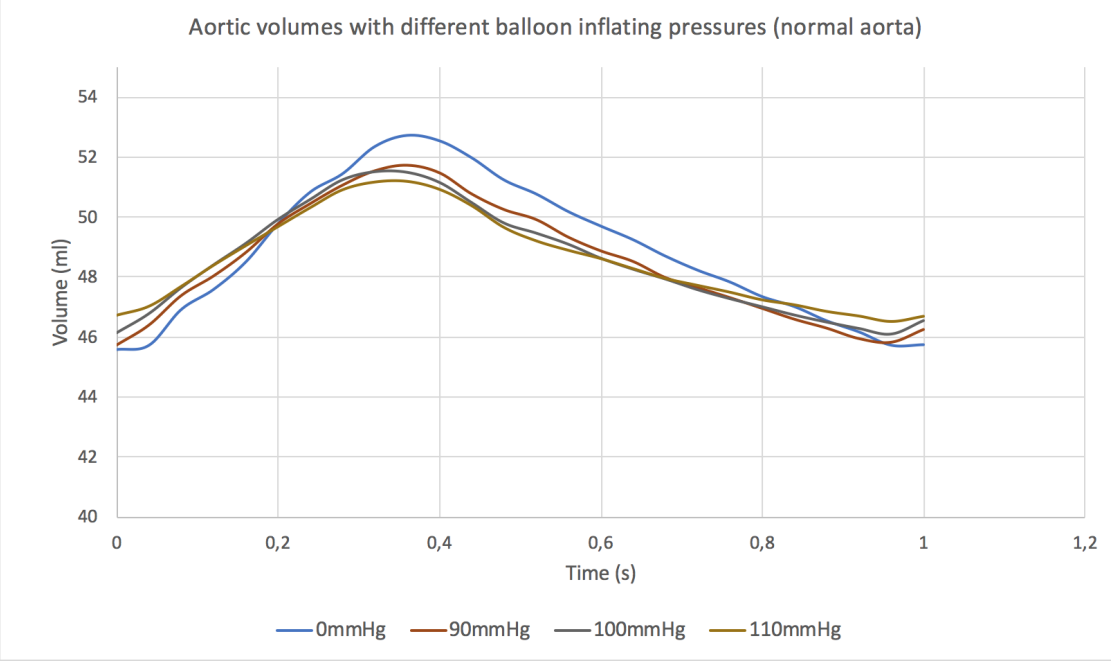

Figure 4.20: Volume mean complexes in function of different balloon inflating pressures.

The diameter values obtained with different balloon inflating pressure are indicated in table

Inflating pressure	**d max ± 0,05**	**d min ± 0,05**	**Δdiam ± 0,1**
mmHg	mm	mm	mm
0	31,20	28,80	2,4
60	31,20	28,80	2,4
70	31,17	28,80	2,4
80	31,04	28,70	2,3
90	30,92	28,70	2,2
100	30,92	28,90	2,0
110	30,56	29,10	1,5
120	30,65	29,00	1,7

Table 4.5: Diameter values obtained for every different inflating pressure condition.

The aortic diameter variations graph for different balloon inflating pressures is represented in fig. 4.21.

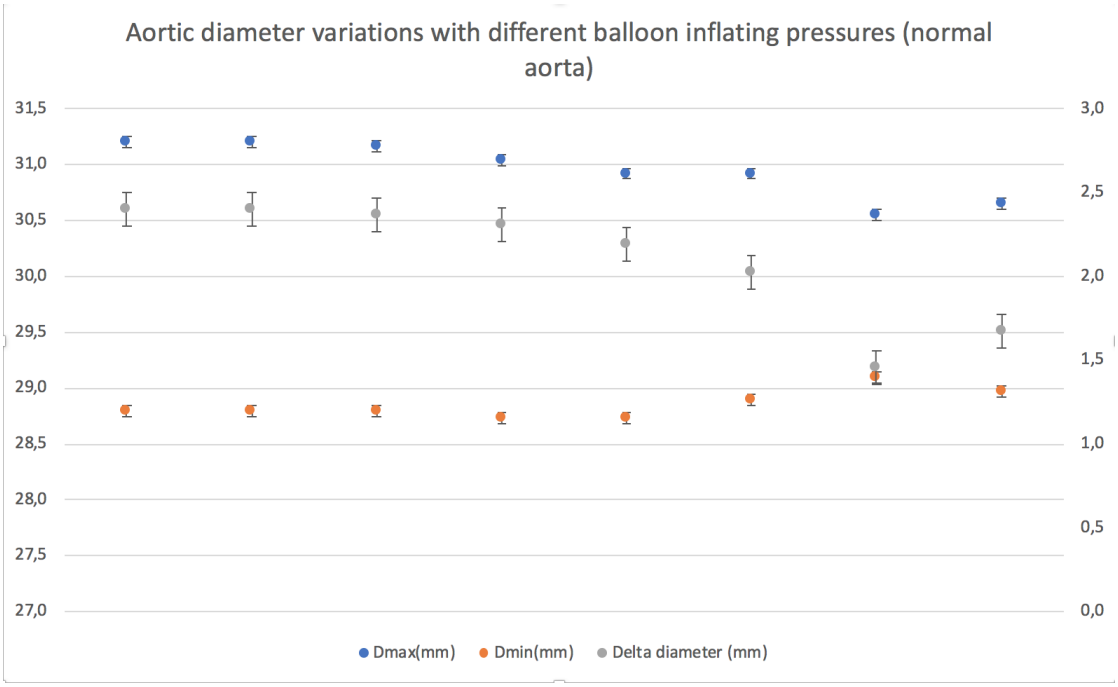

Figure 4.21: Aortic diameter variations trend with different balloon inflating pressures.

Stiffened aorta

Inflating pressure mmHg	Systolic pressure±1 mmHg	Diastolic pressure±1 mmHg	Mean pressure±2 mmHg	Aortic pulse±2 mmHg
0	144	88	107	56
80	145	90	108	55
90	144	90	108	54
100	138	87	104	51
110	137	90	106	47
120	135	92	106	43
130	136	94	108	42
140	136	94	108	42

Table 4.6: Values of systolic pressure, diastolic pressure, mean pressure and aortic pulse for each inflating pressure condition.

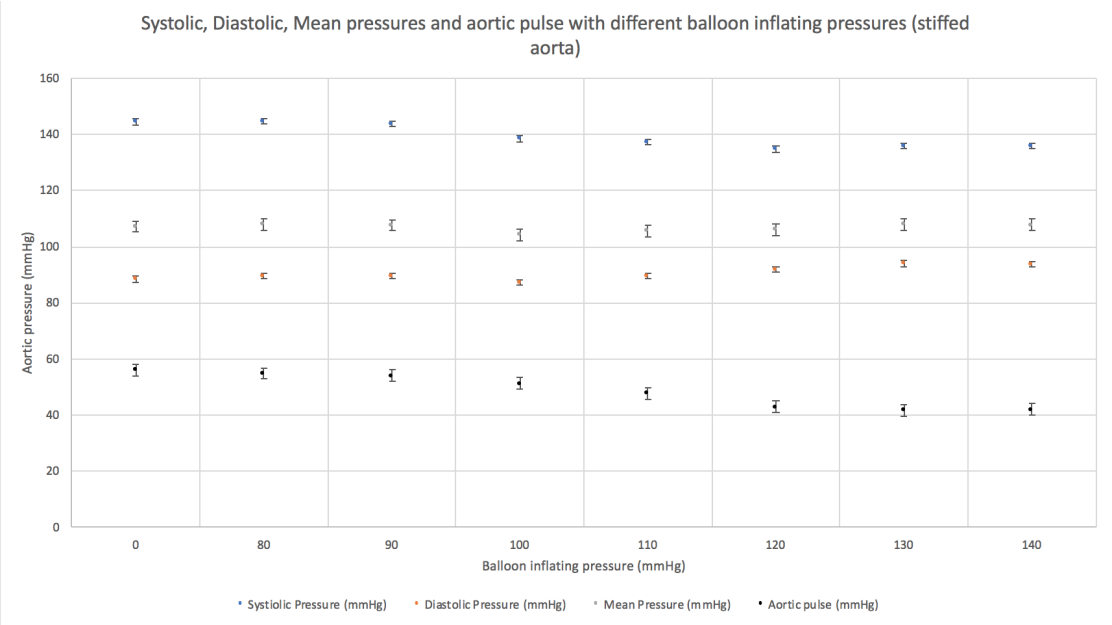

Figure 4.22: Systolic, diastolic, mean pressure trends with different inflating pressure conditions.

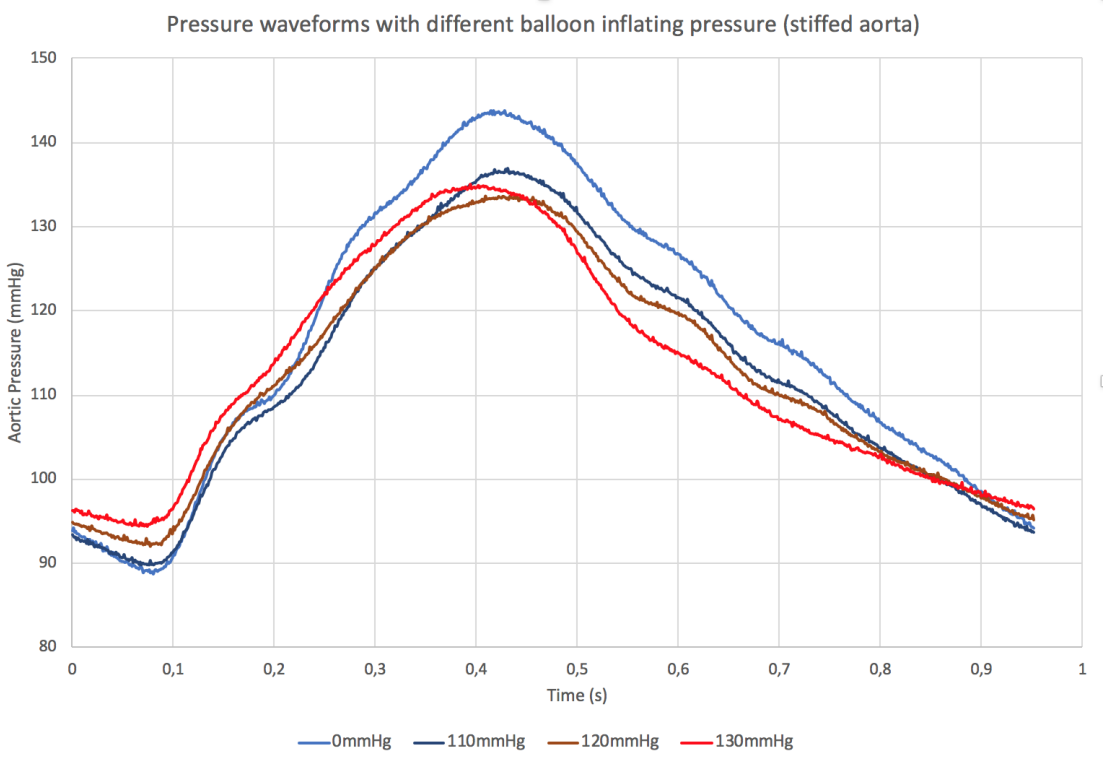

Figure 4.23: Pressure mean complexes in function of different balloon inflating pressures.

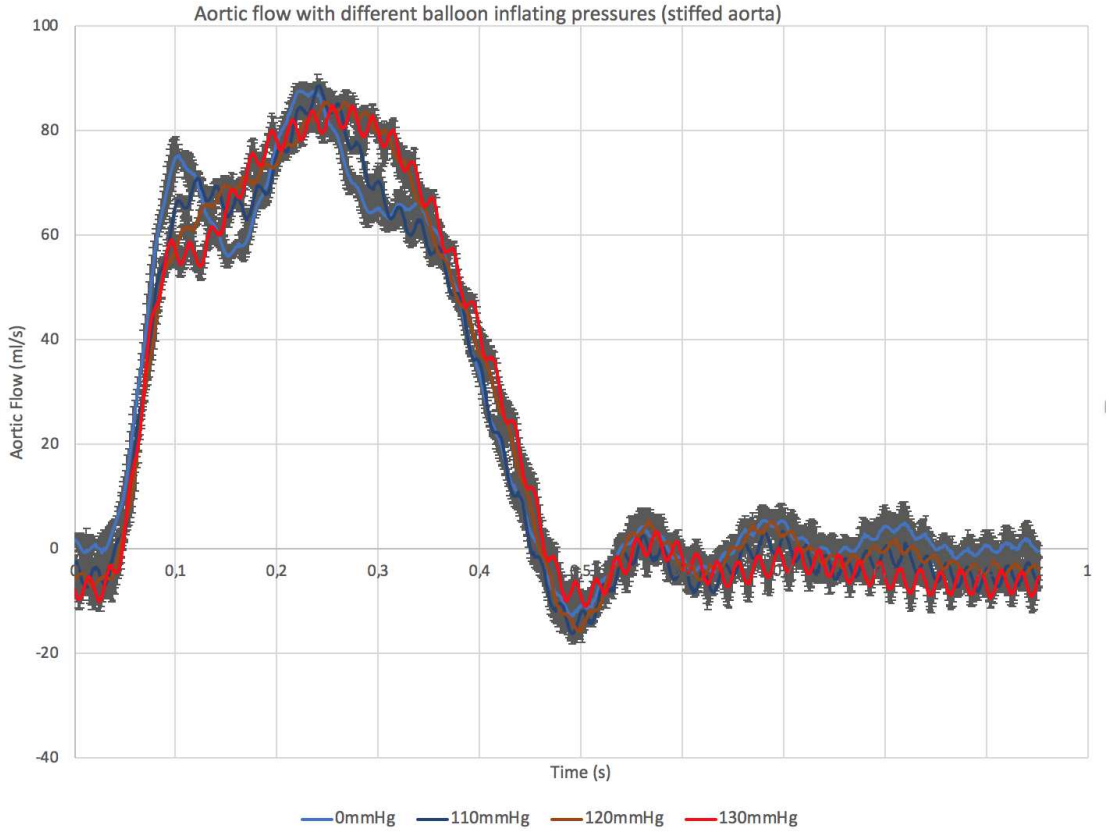

Figure 4.24: Flow mean complexes in function of different balloon inflating pressures.

Inflating pressure	**Max pressure±1**	**Min pressure±1**	**PIABP pulse ±2**
mmHg	mmHg	mmHg	mmHg
0	0	0	0
80	82	82	0
90	90	89	1
100	101	100	1
110	111	109	2
120	118	116	2
130	133	131	2
140	141	139	2

Table 4.7: Maximum and minimum pressure values inside the PIABP.

Inflating pressure	**Vol max ± 0,1**	**Vol min ± 0,1**	**ΔVol ± 0,2**
mmHg	mL	mL	mL
0	67,9	63,1	4,8
80	67,9	63,2	4,7
90	67,9	63,2	4,6
100	67,9	63,1	4,8
110	67,8	63,3	4,5
120	67,8	63,2	4,6
130	67,7	63,4	4,3
140	67,4	63,5	3,9

Table 4.8: Volume values obtained for every different inflating pressure condition.

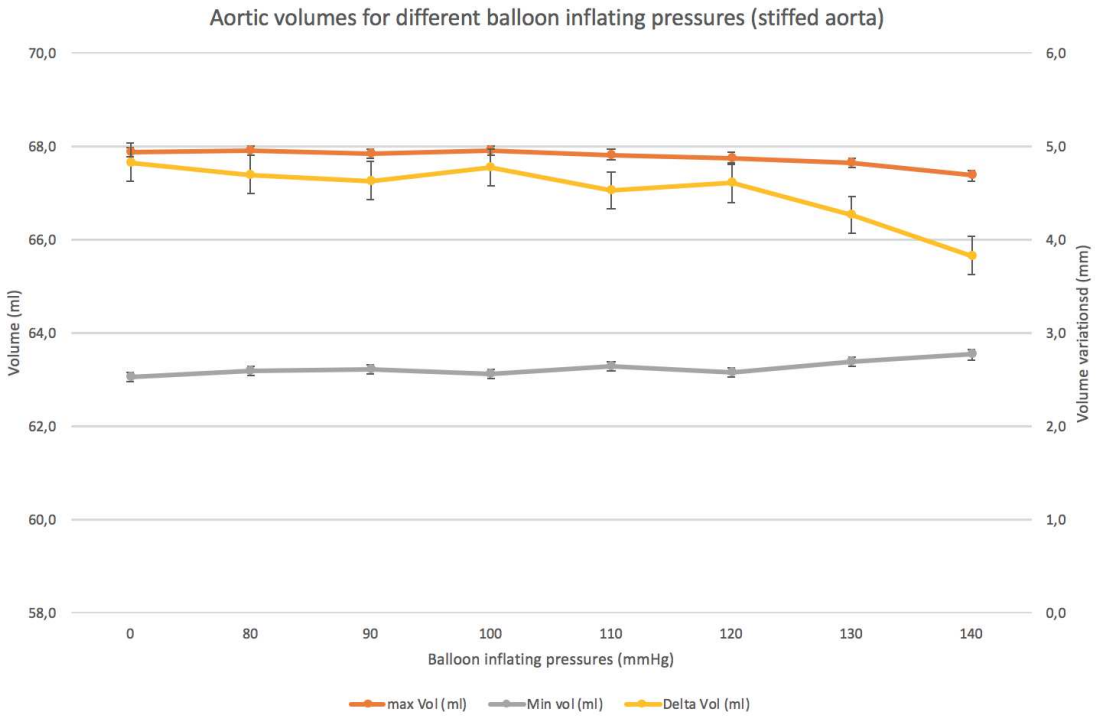

Figure 4.25: Aortic volume trend with different inflating pressures.

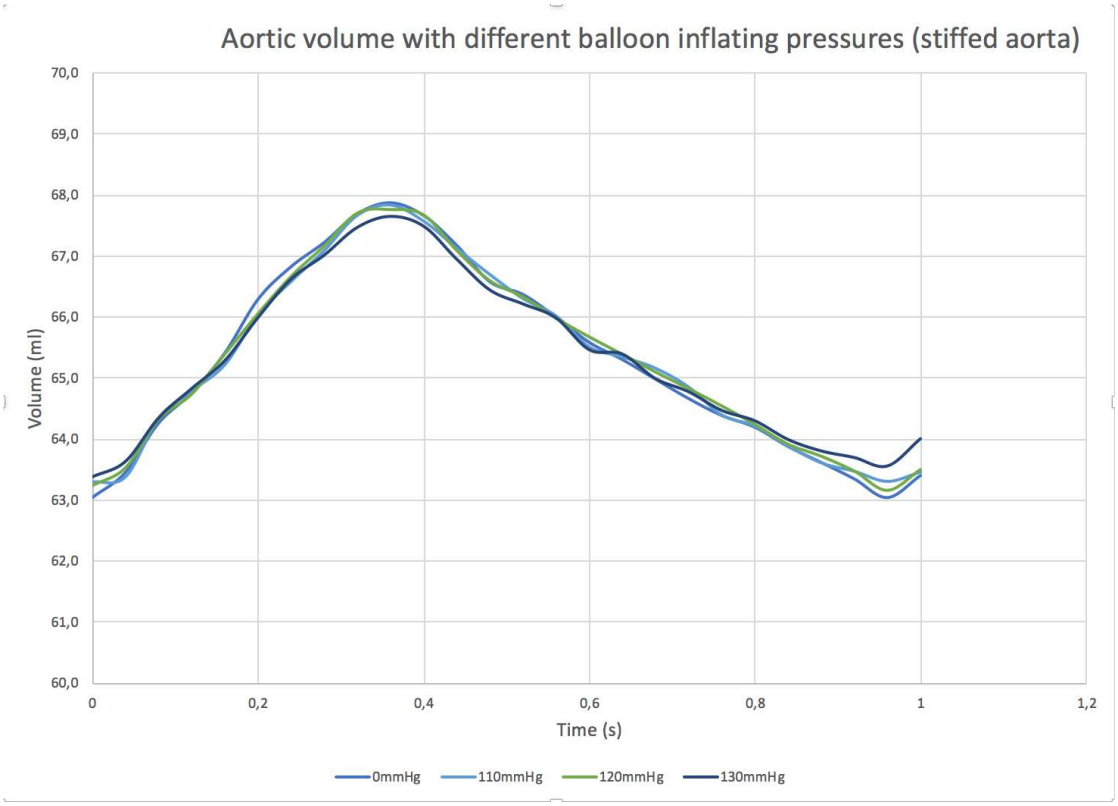

Figure 4.26: Volume mean complexes in function of different balloon inflating pressures.

Inflating pressure	**d max ± 0,05**	**d min ± 0,05**	**Δdiam ± 0,1**
mmHg	mm	mm	mm
0	30,20	29,10	1,1
80	30,20	29,10	1,1
90	30,20	29,10	1,1
100	30,10	29,10	1,0
110	30,20	29,20	1,0
120	30,10	29,30	0,8
130	30,10	29,30	0,8
140	30,20	29,40	0,8

Table 4.9: Diameter values obtained for every different inflating pressure condition.

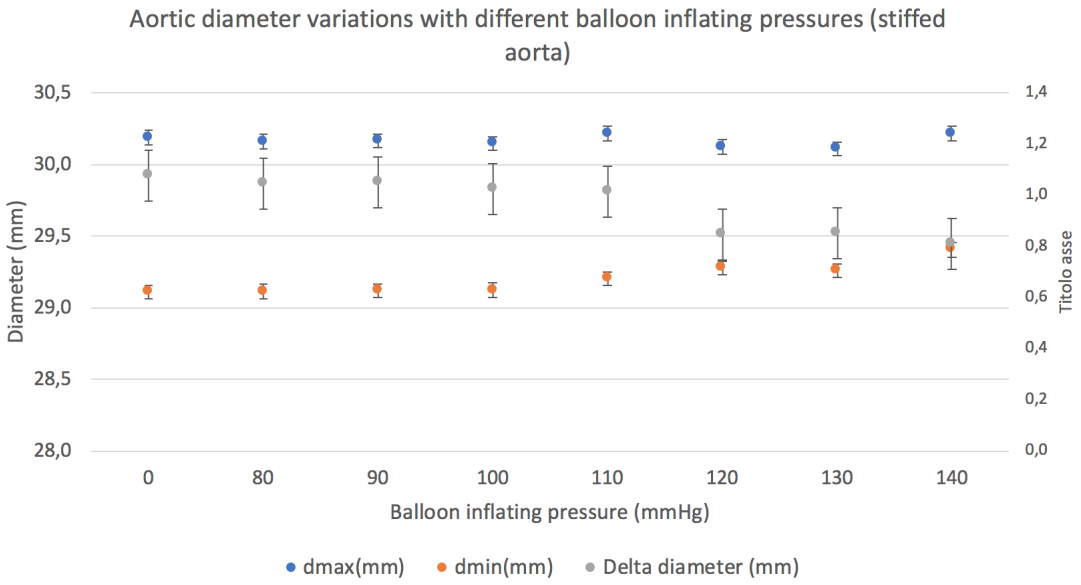

Figure 4.27: Aortic diameter variations trend with different balloon inflating pressures.

Chapter 5

Discussion

Our white aorta correctly simulates the elastic behavior of a healthy subject normal aorta. In fact, a pulse of about 40 *mmHg* the vessel diameters varies of 2,4 *mm*.

By inflating the PIABP, the arterial pulse progressively reduces with a maximal effect with an internal pressure of 110 *mmHg* (a value between the mean pressure and the diastolic pressure.). The pressure in the external reservoir pulses (ΔP is about 8 *mmHg* for the best inflating conditions) and demonstrates the correct functioning of the PIABP.

Aortic volumes and diameters decrease during PIABP inflating and the maximal effect is obtained with an internal pressure of 110 *mmHg*. In this condition the aortic diameter decreases of about 1 *mm*.

The rigid aorta shows a similar behavior of the normal one but with very reduced effects both in term of arterial pressure decrease and volumes/diameters variations (about 0,3 *mm* in the best condition).

This thesis was focused on the effect of passive counterpulsation on the mechanical matching between left ventricle and aorta.

The original goal was to verify this on patients by monitoring, non invasively,

the aortic blood flow signal. The two cases we studied demonstrated an unacceptable variability operator- related and we decided to come back to the mechanical simulator to deep knowledge of the mechanical phenomenon by observing directly, for the first time, the pulsating balloon. For this it was necessary to join a synchronized video recording to the signals monitoring.

The visual observation of the pulsation opened a new interest: recent clinical changes of endovascular therapy, with use of endoprothesis, highlights the problem of contact between the prosthetic wall and the vascular wall, which changes with pressure pulsatility. May the passive counterpulsation be a solution for this problem? We tested it and we demonstrated that this is possible. Now it is matter for clinicians to apply this suggestion or not; we as medical Physicists did our role.

Bibliography

[1] Andreoli TE., Carpenter CGJ., Benjamin IJ., Griggs RC., Wings EJ. *Cecil Essentials of Medicine* ; (8th edn). Saunders Elsevier, 2011.

[2] Bazan O., Ortiz JP. *Experimental validation of a cardiac simulator for in vitro evaluation of prosthetic heart valves*; Braz. J. Cardiovasc. Surg. 31 (2), 2016.

[3] Chien S., Chen PCY., Fung YC. *An Introductory text to bioengineering*; World Scientific, Advanced Series in Biomechanic, Vol.4

[4] Corazza I., Melandri G., Nanni S., Marcelli E., Cercenelli L., Bianchini D., Vagnarelli F., Zannoli R. *Passive counterpulsation: Biomechanical rationale and clinical validation*; Journal of Mechanics in Medicine and Biology 13(5): 134-145, 2013.

[5] Corazza I., Bianchini D., Marcelli E., Cercenelli L., Zannoli R. *Passive aortic counterpulsation: Biomechanical rationale and bench validation*; Journal of Biomechanics, 2014.

[6] Corazza I., Casadei L., Zannoli R. *A simple and innovative way to measure ventricular volume in a mechanical mock of the left ventricle*; Biomechanical Signal and Processing and Control, 2016.

[7] Doost SN., Ghista D., Zhong BSL., Morsi YS. *Heart blood flow simulation: a perspective review*; Biomed. Eng. OnLine 15, 2016.

[8] Eltchaninoff H., Dimas AP., Whitlow PL. *Complications associated with percutaneous placement and use of intraaortic balloon counterpulsation*; Am.J. Cardiol. 71, 328-332.

[9] Kantrowitz A., Tjonneland S., Freed PS., Phillips SJ., Butner AN, Sherman Jr JL. *Initial clinical experience with intraaortic balloon pumpinh in cardiogenic shock*; JAMA 203, 113-118, 1968.

[10] Krishna M., Zacharowky K. *Principles of intra-aortic balloon counterpulsation*; Contin. Educ. Anaesth. Crit. Care Pain 9, 24-28, 2009.

[11] Santa-Cruz RA., Cohen MG., Ohman EM. *Aortic counterpulsation: A review of the hemodynamic effects and indications for use*; Catheter Cardiovasc. Interv 67:68-77, 2006.

[12] Suga, H. *Time course of left ventricular pressure-volume relationship under various end-diastolic volume.* Jap ,Heart J 10:509-515, 1969 .

[13] Suga, H. *Left ventricular pressure-volume ratio in systole as an index of myocardial inotropism.* Jap Heart J 12:153-160, 1971.

[14] Sagawa *The ventricular pressure-volume diagram revisited.* An official journal of American Haert Association, 1978.

[15] www.maquet.com.

[16] Zannoli R., Corazza I, Branzi A. *Mechanical simulator of the cardiovascular system.* Journal of mechanics in medicine and biology, (2005).

[17] Zannoli R., Corazza I., Branzi A., Rossi PL *Aortoventricular mechanical matching: Simulation of normal and pathological conditions*; J Mech Med Biol 8:12, 2008.

[18] Zannoli R., Corazza I, Cacciafesta P., Branzi A. *Evaluating the mechanical behavior of a ventricular simulator*. Physica Medica, (2009).